Myeloid cells, BAFF, and IFN-γ establish an inflammatory loop that exacerbates autoimmunity in Lyn-deficient mice

Patrizia Scapini,[1] Yongmei Hu,[1] Ching-Liang Chu,[3] Thi-Sau Migone,[4] Anthony L. DeFranco,[2] Marco A. Cassatella,[5] and Clifford A. Lowell[1]

[1]Department of Laboratory Medicine and [2]Department of Microbiology/Immunology, University of California, San Francisco, San Francisco, CA 94143
[3]Immunology Research Center, National Health Research Institutes, Miaoli County 350, Taiwan
[4]Human Genome Sciences, Inc., Rockville, MD 20850
[5]Department of Pathology, Section of General Pathology, University of Verona, 37134 Verona, Italy

Autoimmunity is traditionally attributed to altered lymphoid cell selection and/or tolerance, whereas the contribution of innate immune cells is less well understood. Autoimmunity is also associated with increased levels of B cell–activating factor of the TNF family (BAFF; also known as B lymphocyte stimulator), a cytokine that promotes survival of self-reactive B cell clones. We describe an important role for myeloid cells in autoimmune disease progression. Using Lyn-deficient mice, we show that overproduction of BAFF by hyperactive myeloid cells contributes to inflammation and autoimmunity in part by acting directly on T cells to induce the release of IFN-γ. Genetic deletion of IFN-γ or reduction of BAFF activity, achieved by either reducing myeloid cell hyperproduction or by treating with an anti-BAFF monoclonal antibody, reduced disease development in *lyn*$^{-/-}$ mice. The increased production of IFN-γ in *lyn*$^{-/-}$ mice feeds back on the myeloid cells to further stimulate BAFF release. Expression of BAFF receptor on T cells was required for their full activation and IFN-γ release. Overall, our data suggest that the reciprocal production of BAFF and IFN-γ establishes an inflammatory loop between myeloid cells and T cells that exacerbates autoimmunity in this model. Our findings uncover an important pathological role of BAFF in autoimmune disorders.

CORRESPONDENCE
Clifford A. Lowell:
clifford.lowell@ucsf.edu

Abbreviations used: AFC, antibody-forming cell; ANA, antinuclear antibody; BAFF, B cell–activating factor of the TNF family; BMD, bone marrow derived; C3, complement factor 3; TLR, Toll-like receptor.

Systemic lupus erythematosus is a prototypic autoimmune disease with complex and unclear etiology (Rahman and Isenberg, 2008). Most studies of this disease have focused on the defects of B and T cell tolerance as an underlying cause of the disorder. Recently, however, greater attention has been given to the pathological roles of myeloid cells in autoimmunity (Cohen et al., 2002; Hanada et al., 2003; Zhu et al., 2005; Stranges et al., 2007).

Mice lacking Lyn, an Src family kinase mainly expressed in B and myeloid cells, are a well-established model of lupus-like autoimmunity (Xu et al., 2005). *lyn*$^{-/-}$ mice develop progressive autoimmunity characterized by autoantibody production, lymphocyte activation, immune complex deposition, and nephritis (Hibbs et al., 1995; Nishizumi et al., 1995; Chan et al., 1997; Yu et al., 2001). The development of autoimmunity in *lyn*$^{-/-}$ mice has been mainly attributed to alterations in B cell signaling thresholds, leading to abnormal B cell selection and/or tolerance resulting in production of self-reactive antibodies (Chan et al., 1998; Xu et al., 2005). The Lyn mutation directly affects B cell development, as *lyn*$^{-/-}$ mice have an ∼30–50% reduction in mature B cell numbers because of the reduction of specific B cell subtypes such as marginal zone and follicular B cells (Xu et al., 2005; Gross et al., 2009).

Lyn is also expressed in innate immune cells, where it regulates cell signaling thresholds to several CSFs, such as G-CSF, GM-CSF, and M-CSF (Harder et al., 2001, 2004; Scapini et al., 2009). *lyn*$^{-/-}$ myeloid cells are hyperresponsive

The Rockefeller University Press $30.00
J. Exp. Med. Vol. 207 No. 8 1757-1773
www.jem.org/cgi/doi/10.1084/jem.20100086

to engagement of surface integrins, leading to hyperadhesion, enhanced respiratory burst, and increased secondary granule release (Pereira and Lowell, 2003). Despite this experimental evidence in vitro, the contribution of myeloid cells to the development of autoimmunity in *lyn*$^{-/-}$ mice has not been investigated.

Autoimmunity is often associated, both in mice and humans, with excess production of B cell–activating factor of the TNF family (BAFF), a member of the TNF superfamily of cytokines also known as B lymphocyte stimulator (Mackay et al., 2007; Stadanlick and Cancro, 2008; Mackay and Schneider, 2009). Both autoimmune-prone mice (such as MRL$^{lpr/lpr}$ and NZB×W F1) and human patients suffering from autoimmune disorders such as systemic lupus erythematosus or rheumatoid arthritis have elevated serum levels of BAFF (Kalled, 2005; Mackay and Schneider, 2009). This cytokine is thought to exert its pathogenic role, under conditions of excess production, through its ability to support survival and proliferation of autoreactive B cells, which have a higher BAFF dependence (Lesley et al., 2004). However, in addition to its effect on B cells, recent work has suggested that BAFF can also promote T cell activation (Ye et al., 2004; Sutherland et al., 2005; Mackay and Leung, 2006; Lai Kwan Lam et al., 2008). Despite this evidence, it remains unclear if BAFF exerts a direct pathogenic role on T cells in vivo during autoimmunity. Furthermore, the mechanisms responsible for deregulated BAFF production in autoimmune diseases have been poorly investigated. Studies in mice have shown that there are two distinct pools of BAFF: a constitutive pool produced by stromal cells, which is thought to regulate the size and maturation stage of the peripheral B cell compartment, and an accessory pool, produced mainly by myeloid cells during inflammatory or immune responses (Schneider, 2005). Which of these two pools contributes to autoimmune pathologies is unknown. Different attempts to neutralize BAFF activity in autoimmune disorders have been performed in both mice and humans, but despite a general agreement on the efficacy of the treatments, the mechanisms of this protection are still not fully understood (Ding, 2008; Ramanujam and Davidson, 2008; Moisini and Davidson, 2009).

Another important cytokine that has been shown to be involved in lupus pathogenesis is IFN-γ. Several studies in MRL$^{lpr/lpr}$ and NZB×W F1 autoimmune-prone mice observed significant reduction of histological and serological disease characteristics, and extended survival in these strains after IFN-γ genetic deletion or after anti–IFN-γ mAb treatment (Theofilopoulos et al., 2001).

We found that the levels of BAFF were dramatically higher in the sera of *lyn*$^{-/-}$ mice compared with WT animals, and that the deregulated production of BAFF by *lyn*$^{-/-}$ myeloid cells can contribute to autoimmunity in these animals by affecting not only B cell activation but, more interestingly, by directly promoting T cell activation and IFN-γ production by the latter cells. These findings shed new insight on the pathological mechanisms of interplay between innate and adaptive immunity, as well as the consequences of BAFF and IFN-γ overproduction, in autoimmune disorders.

RESULTS

Lyn-deficient myeloid cells overproduce BAFF

As seen in other autoimmune-prone mice, the serum levels of BAFF were significantly elevated in *lyn*$^{-/-}$ mice at 2 mo of age and progressively increased over time, reaching 3.1–4.8 times the WT levels (Fig. 1 A). The increased BAFF serum levels in young *lyn*$^{-/-}$ mice could be a consequence of the ∼30–50% reduction in mature B cell numbers caused by Lyn deficiency (Xu et al., 2005); however, this did not explain the progressive rise in BAFF with age, which is likely caused by overproduction of the cytokine by *lyn*$^{-/-}$ myeloid cells. Indeed, starting between 3–4 mo of age *lyn*$^{-/-}$ mice manifested progressive myeloproliferation (Fig. 1 B), culminating at ∼10 mo of age in a dramatic expansion of granulocyte (Mac-1^{high}7/4^{int}GR-1^{high}), monocyte (Mac-1^{high}7/4^{high}GR-1^{low}), macrophage (F4/80^{+}), and DCs (CD11c^{+}) compartments (Fig. S1 A). Correlated with the myeloid expansion, the levels of BAFF mRNA expression in total spleen or sorted splenic macrophages/DCs from *lyn*$^{-/-}$ mice (age 6–8 mo) were elevated (Fig. 1 C). Notably, there was no significant increase of BAFF mRNA expression in the spleens of young *lyn*$^{-/-}$ mice before the onset of myeloproliferation (unpublished data), indicating that expansion/activation of myeloid cells and not stromal cells (Lesley et al., 2004) is likely responsible for the increased splenic BAFF mRNA expression observed in old *lyn*$^{-/-}$ mice. In line with these findings, we observed that cultured bone marrow–derived (BMD) macrophages and DCs from *lyn*$^{-/-}$ mice overproduced BAFF, as assessed at both the mRNA and protein level, primarily in response to IFN-γ stimulation (Fig. 1, D and E). In combination with M-CSF and GM-CSF, IFN-γ induced even higher release of BAFF without altering mRNA levels (Fig. 1, D and E) because of the proliferative effects of these CSFs (as confirmed by proliferation assays run in parallel; not depicted). These data suggest that the overproduction of BAFF by *lyn*$^{-/-}$ macrophages and DCs in vivo is likely caused by both increased proliferation and exaggerated responses to IFN-γ. Indeed, in vitro, *lyn*$^{-/-}$ macrophages and DCs demonstrated increased STAT-1 phosphorylation and IP-10/CXCL10 production after IFN-γ stimulation (Fig. S1, B and C). Neutrophils are also a known source of BAFF (Scapini et al., 2008); indeed, Lyn-deficient BMD neutrophils released higher levels of BAFF than WT neutrophils in response to proinflammatory mediators such as fMLP, TNF, and IFN-γ but not to PMA, which activates neutrophils independently of Src family kinases (Fig. S1 D). These data suggest that besides splenic macrophages and DCs, other myeloid cell types (granulocytes and monocytes) present in the spleens of old *lyn*$^{-/-}$ mice might contribute to the observed increased BAFF mRNA expression in the total spleen. In contrast, there was no difference in the low levels of BAFF mRNA present in T cells from WT versus *lyn*$^{-/-}$ mice (unpublished data). The BAFF protein released by *lyn*$^{-/-}$ myeloid cells was biologically active because it supported B cell survival in vitro (Fig. S2). These data demonstrate that overproduction of BAFF by hyperactive *lyn*$^{-/-}$ myeloid cells may be responsible for the progressive increase in serum BAFF observed over time in *lyn*$^{-/-}$ mice.

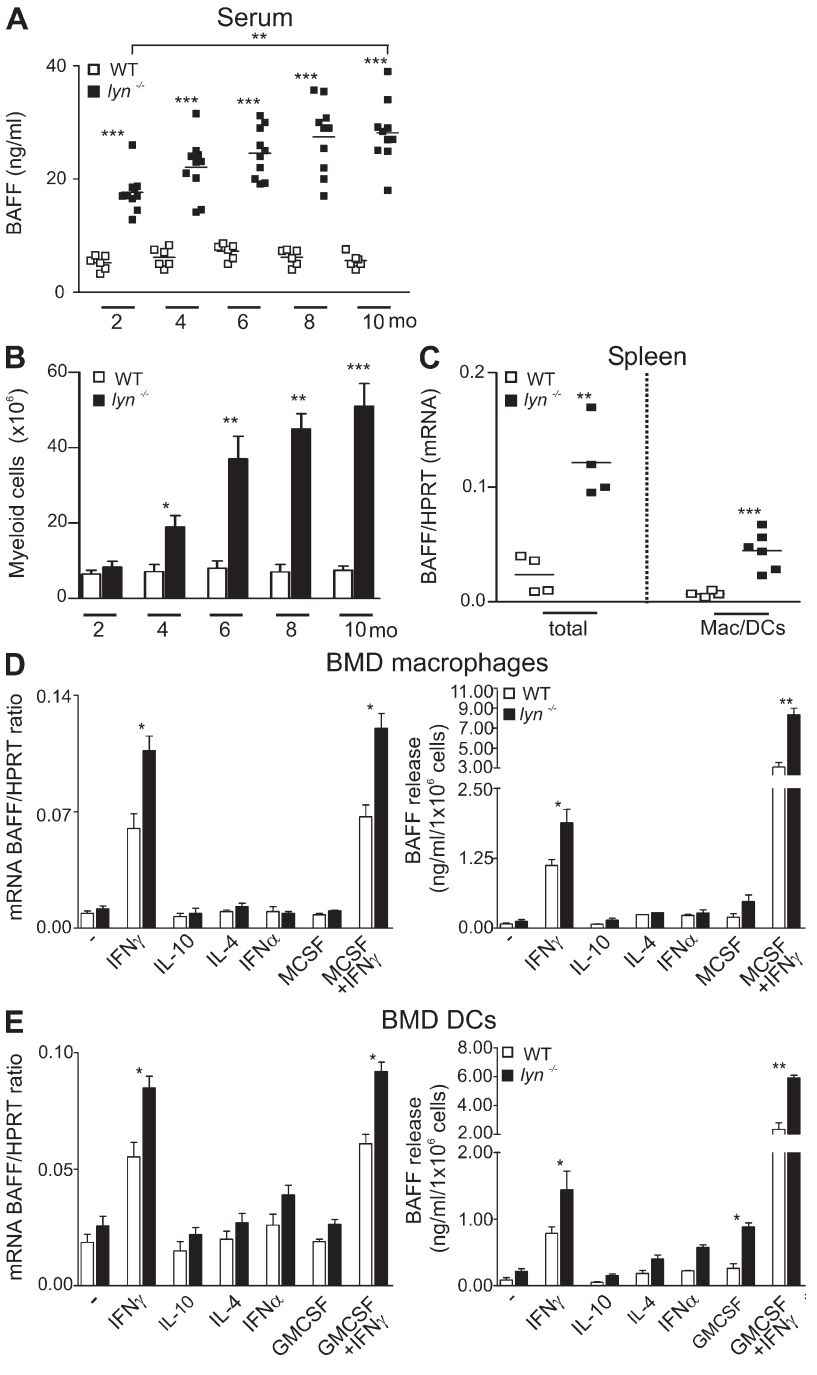

Figure 1. Increased BAFF production by *lyn*$^{-/-}$ myeloid cells in vivo and in vitro. (A) ELISA of BAFF serum levels in WT and *lyn*$^{-/-}$ mice. Statistical differences in BAFF serum levels between WT and *lyn*$^{-/-}$ mice are indicated at each time point. Statistical differences in serum BAFF between 2- and 10-mo-old *lyn*$^{-/-}$ mice are also reported. Each symbol represents the BAFF serum level of an individual mouse. Horizontal bars represent means. Data are representative of two independent kinetic experiments. (B) Single-cell suspensions of spleens from WT or *lyn*$^{-/-}$ mice at different ages were prepared, counted, and stained for FACS analysis. The total number of Mac-1^{+} myeloid cells is reported. Data are expressed as means ± SEM (n = 6–10 mice per time point). Data are pooled from two separate kinetic experiments. (C) BAFF mRNA expression in total spleen or sorted splenic macrophages and DCs (F4/80^{+}CD11c^{+}) from 6–8-mo-old WT or *lyn*$^{-/-}$ mice. Horizontal bars represent means. Data are representative of one end-point experiment (n = 4–6). (D and E) BAFF mRNA expression and protein release in vitro by BMD macrophages or BMD DCs, prepared as described in Materials and methods from 2–3-mo-old WT or *lyn*$^{-/-}$ mice, were determined by quantitative RT-PCR and ELISA, respectively. BAFF mRNA expression (24 h; left) and protein release (48 h; right) by BMD macrophages (D) or BMD DCs (E) in response to the indicated stimuli. Means ± SEM of data from four to six independent experiments are reported. *, $P < 0.05$; **, $P < 0.01$; ***, $P < 0.001$.

Increased IFN-γ production by activated T cells in *lyn*$^{-/-}$ mice

Given that IFN-γ proved to be the major inducer of BAFF production by *lyn*$^{-/-}$ macrophages and DCs in vitro, we examined the levels of this cytokine in vivo. *lyn*$^{-/-}$ mice manifested a progressive increase in serum levels of IFN-γ, which began to rise between 3 and 4 mo of age coincident with rising BAFF levels (Fig. 2 A). By 6–8 mo of age, *lyn*$^{-/-}$ mice displayed dramatically elevated splenic IFN-γ mRNA compared with WT animals (Fig. 2 B). Coincident with the rise in these cytokines, the numbers of activated (CD69^{+}) and effector (CD44^{high} CD62L^{-}) T cells (of both the CD4 and CD8 subtypes) in the spleens of *lyn*$^{-/-}$ animals also progressively increased (Fig. 2 C, left; and Fig. 2 D, top and middle). Most importantly, a large number of the activated T cells (of both the CD4 and CD8 subtypes) were producing IFN-γ (Fig. 2 C, right; and Fig. 2 D, bottom). Because Lyn kinase is not expressed in the T cell lineage, the development of progressive T cell activation and IFN-γ production in *lyn*$^{-/-}$ mice must be caused by some non–T cell factor that is acting on these cells. Collectively, these initial findings suggested that there was a strong kinetic correlation between a progressive increase in myeloproliferation, T cell activation, BAFF, and IFN-γ overproduction in *lyn*$^{-/-}$ mice. Interestingly, the lymph nodes of the *lyn*$^{-/-}$ mice did not display evidence of myeloid cell accumulation and had lower numbers of activated T cells compared with the spleen.

Block in myeloid cell activation/proliferation by the deficiency of Hck and Fgr reduces BAFF production and T cell activation in *lyn*$^{-/-}$ mice

To understand the contribution of myeloid cell hyperactivation/proliferation to the elevated serum BAFF and IFN-γ as

well as to the autoimmunity in *lyn*$^{-/-}$ mice, we investigated how reduction in myeloid cell expansion/activation would affect these phenomena. For this purpose, we analyzed the phenotype of Hck/Fgr/Lyn triple-deficient (*HFL*$^{-/-}$) mice. These three kinases make up the primary Src family members expressed in myeloid leukocytes; however, they play different roles, with Lyn being predominantly a negative regulator of myeloid cell reactivity, whereas Hck and Fgr contribute to positive signaling (Lowell, 2004; Berton et al., 2005; Scapini et al., 2009). Myeloid cells lacking all three of these kinases show a hypoproliferative phenotype in response to cytokine stimulation in vitro because of impaired STAT phosphorylation (unpublished data; Rane and Reddy, 2002). As a result, the *HFL*$^{-/-}$ mice themselves lack the severe splenomegaly and myeloproliferation (in particular of macrophages and DCs) seen in the *lyn*$^{-/-}$ animals (Fig. 3, A and B, left; and Fig. S3 A), whereas the total number of B and T cells was similar (Fig. 3 B, left). These mice therefore served as an important model to test if reduction in myeloproliferation would affect BAFF, IFN-γ, and autoimmune progression. The *HFL*$^{-/-}$ mice showed elevated BAFF levels early in life, similar to the *lyn*$^{-/-}$ animals and consistent with the B cell lymphopenia in both strains; however, the *HFL*$^{-/-}$ strain failed to manifest the progressive rise in serum BAFF seen in the single mutant *lyn*$^{-/-}$ animals (Fig. 3 C). BAFF mRNA levels in splenic macrophages and DCs (or total spleen cells) was dramatically lower in the *HFL*$^{-/-}$ mice compared with the *lyn*$^{-/-}$ animals (Fig. 3 D, left). The *HFL*$^{-/-}$ mice also had significantly lower numbers of activated T cells, lower numbers of IFN-γ–producing T cells, and lower amounts of splenic IFN-γ mRNA (Fig. 3, B and D, right), despite the fact that none of these kinases are present in T cells. On the other hand, the activated B cell phenotype (including the enhanced expression of co-stimulatory molecules) was largely unchanged in *HFL*$^{-/-}$ compared with *lyn*$^{-/-}$ mice, in line with the fact that Hck and Fgr are not expressed in most B cell types (Fig. 3 B, right; and Fig. S3 B). Furthermore, the hyperactive B cells in the *HFL*$^{-/-}$ animals produced levels of total Ig and autoreactive anti-dsDNA and anti-RNA antibodies at levels just below the single mutant *lyn*$^{-/-}$ mice (Fig. S3 C and not depicted). A more detailed characterization of the autoantibodies present in the sera of *HFL*$^{-/-}$ mice revealed that, similar to *lyn*$^{-/-}$ mice, IgG2a/c was the main pathogenic isotype for both anti-dsDNA and anti-RNA antibodies (Fig. S3 C and not depicted). Furthermore, the serum of both *HFL*$^{-/-}$ and *lyn*$^{-/-}$ mice contained high levels of antinuclear autoantibodies (ANAs), which displayed strong nuclear homogeneous and nuclear speckled staining patterns, indicative of both anti-DNA and anti-RNA antibodies (Fig. S3 D). The reduction in myeloproliferation and T cell activation correlated

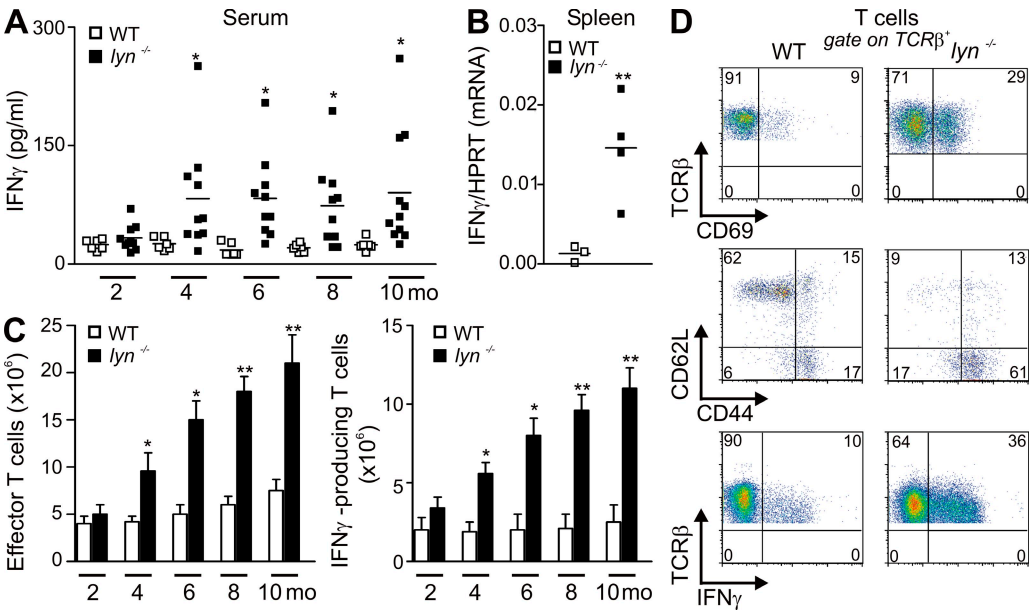

Figure 2. Progressive increase in T cell activation and IFN-γ production in aging *lyn*$^{-/-}$ mice. (A) IFN-γ serum levels in WT and *lyn*$^{-/-}$ mice were assessed by ELISA. Each symbol represents the IFN-γ serum level of an individual mouse. Horizontal bars represent means. Data are pooled from three independent kinetic experiments (n = 6–10). (B) IFN-γ mRNA expression in total spleens from of 6–8-mo-old WT or *lyn*$^{-/-}$ mice. Horizontal bars represent means. Data are representative of one end-point experiment (n = 3–4). (C and D) Single-cell suspensions of spleens from WT or *lyn*$^{-/-}$ mice at different ages were prepared, counted, and stained for FACS analysis. (C) Total number of TCRβ^{+}CD44^{high}CD62L^{-} (effector cells; left) and TCRβ^{+}IFN-γ^{+} (IFN-γ–producing cells; right) are reported as evidence of T cell activation. The number and percentage of IFN-γ–producing T cells were evaluated by intracellular staining after ex vivo stimulation of splenocytes with PMA plus ionomycin for 4 h. Data are expressed as means ± SEM (n = 6–10 mice per time point). Data are pooled from two independent kinetic experiments. *, $P < 0.05$; **, $P < 0.01$. (D) Representative FACS plots demonstrating T cell activation in 10-mo-old *lyn*$^{-/-}$ mice by analysis of the expression of CD69, CD44, CD62L, and IFN-γ are reported. Data are representative of >40 mice for each genotype analyzed at end-point experiments.

with a dramatic reduction in nephritis (interstitial nephritis more than reduced glomerulonephritis) in *HFL*$^{-/-}$ mice (Fig. S3 E). Compared with *lyn*$^{-/-}$ mice, *HFL*$^{-/-}$ animals showed reduced numbers of Mac-1^{+} myeloid cells (mainly macrophages and DCs) and activated T cells infiltrating the kidneys (Fig. 3 E and Table I), despite the fact that glomerular IgG immune complex and complement factor 3 (C3) deposits were still evident, albeit at reduced levels (Fig. S3 F and Table I). The latter were probably responsible for a smaller reduction in glomerulonephritis than in interstitial nephritis in *HFL*$^{-/-}$ mice as compared with *lyn*$^{-/-}$ mice. The renal expression of BAFF and IFN-γ mRNAs was also strongly reduced in the kidneys of *HFL*$^{-/-}$ mice as compared with *lyn*$^{-/-}$ mice (Fig. 3 F). These data demonstrate that a reduction of myeloid cell hyperreactivity in *lyn*$^{-/-}$ mice, achieved by removal of additional Src family kinases, leads to reduction in serum BAFF, T cell activation, IFN-γ production, and nephritis.

Myeloid-specific Lyn deficiency is sufficient to induce BAFF overproduction and autoimmunity

To further explore the interrelationship between myeloproliferation, BAFF, IFN-γ, and autoimmune nephritis, we generated chimeric mice lacking Lyn kinase specifically in myeloid

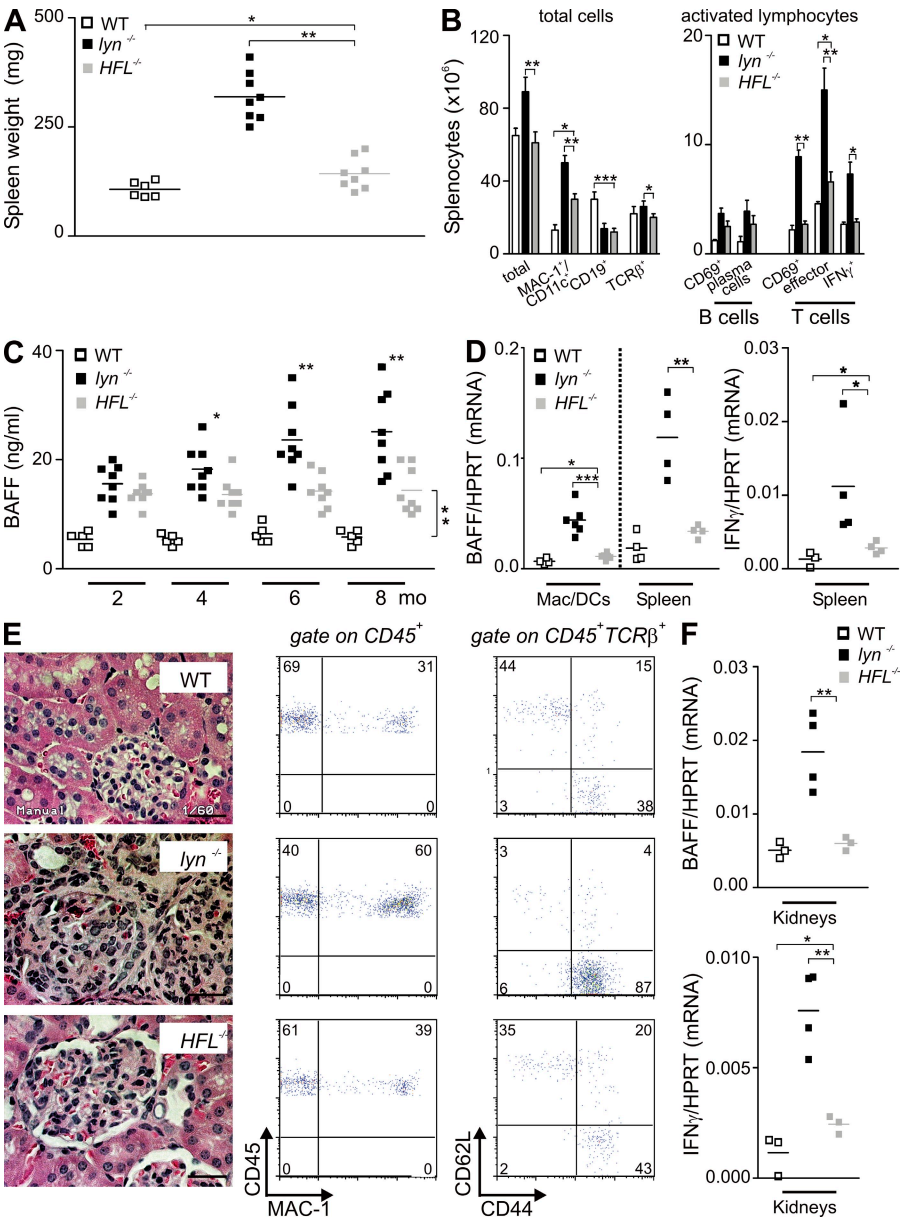

Figure 3. Hck and Fgr deficiency reduces BAFF serum levels, blocks splenomegaly, and improves nephritis in *lyn*$^{-/-}$ mice. (A) Each symbol represents the weight of an individual spleen from 8–10-mo-old WT, *lyn*$^{-/-}$, or *HFL*$^{-/-}$ animals. Horizontal bars represent means. Data are pooled from two independent end-point experiments (n = 6–8). (B) Single-cell suspensions of spleens from 8–10-mo-old WT, *lyn*$^{-/-}$, or *HFL*$^{-/-}$ mice were counted and stained for FACS analysis. (left) The absolute number of total, myeloid plus DC (Mac1^{+}CD11c^{+}), B (CD19^{+}), and T (TCRβ^{+}) cells. (right) The absolute number of activated lymphocytes, CD19^{+}CD69^{+} and CD19/B220$^{int/null}$CD138^{+}, are reported as evidence of B cell activation, whereas TCRβ^{+}CD69^{+}, TCRβ^{+}CD44^{high}CD62L^{-} (effector cells), and TCRβ^{+}IFN-γ^{+} (IFN-γ–producing cells, evaluated as described in Fig. 2) cells are reported as evidence of T cell activation. Data are expressed as means ± SEM (n = 8 mice per group). Statistical differences of *HFL*$^{-/-}$ versus *lyn*$^{-/-}$ mice or *HFL*$^{-/-}$ versus WT mice are reported. Data are pooled from two independent end-point experiments. (C) BAFF serum levels in WT, *lyn*$^{-/-}$, or *HFL*$^{-/-}$ mice assessed by ELISA. Horizontal bars represent means. Data are pooled from two independent kinetic experiments (n = 5–8). (D) BAFF (left) and IFN-γ (right) mRNA expression in sorted splenic macrophages and DCs (F4/80^{+}CD11c^{+}) or total spleens from 6–8-mo-old WT, *lyn*$^{-/-}$, or *HFL*$^{-/-}$ mice. Horizontal bars represent means. Data are representative of one end-point experiment (n = 4–6). (E, left) Representative H&E staining of kidney sections from 8–10-mo-old WT, *lyn*$^{-/-}$, or *HFL*$^{-/-}$ mice. Bars, 100 µm. (middle and right) Representative FACS plot analysis of CD45^{+} myeloid cells (Mac-1^{+}; middle) and activated/effector T cells (CD44^{high}CD62L^{-}) infiltrating the kidneys of 8–10-mo-old WT, *lyn*$^{-/-}$, or *HFL*$^{-/-}$ mice are reported (right). Data are representative of 10–12 mice for each genotype analyzed at end-point experiments. (F) BAFF (top) and IFN-γ (bottom) mRNA expression in total kidneys from 8–10-mo-old WT, *lyn*$^{-/-}$, or *HFL*$^{-/-}$ mice. Data are representative of one independent end-point experiment (n = 3–4). *, P < 0.05; **, P < 0.01; ***, P < 0.001.

Table I. Increased infiltration of leukocytes into the kidneys of *lyn*$^{-/-}$ mice and *lyn*$^{-/-}$*rag*$^{-/-}$ chimeras

	Regular mice				Bone marrow chimeras		
Genotype	**WT**	***lyn*$^{-/-}$**	***HFL*$^{-/-}$**	***lyn*$^{-/-}$ *IFNγ*$^{-/-}$**	**WT**	***rag*$^{-/-}$**	***lyn*$^{-/-}$*rag*$^{-/-}$**
CD45$^+$ (×10^5)	7.5 ± 1.5	22 ± 3	9.5 ± 1***	10.7 ± 1***	8.2 ± 1.7	9.7 ± 1	15.5 ± 1**
CD45$^+$CD19$^+$ (×10^5)	2 ± 0.4	0.9 ± 0.4	1.5 ± 0.5	1 ± 0.3	1.9 ± 0.2	1.2 ± 0.1	1 ± 0.1
CD45$^+$Mac-1$^+$ (×10^5)	3 ± 0.6	15 ± 2	4 ± 1***	5.6 ± 1***	3. ± 0.3	4 ± 0.3	9.2 ± 1**
CD45$^+$TCRβ$^+$ (×10^5)	2.5 ± 0.5	6 ± 1	3.5 ± 0.6*	4 ± 0.6*	3.2 ± 0.6	4.2 ± 0.6	5.1 ± 0.7
CD45$^+$TCRβ$^+$CD44^{high}CD62L$^-$ (%)	35 ± 4	80 ± 5	45 ± 5***	50 ± 3***	42 ± 3	51 ± 6	75 ± 5**
Histological score							
Glomerulonephritis	0	2.8 ± 0.1	1.7 ± 0.1**	1.1 ± 0.2***	0	0.6 ± 0.1	1.6 ± 0.12*
Interstitial nephritis	0	2.5 ± 0.2	1.1 ± 0.1***	0.5 ± 0.1***	0	0.2 ± 0.04	2.3 ± 0.2**
Immunofluorescence staining intensity							
IgM deposit score	+/−	+++	+++	+++	+/−	++	+++
IgG deposit score	−	++	+	+/−	-	-	−
C3 deposit score	−	+++	+	+/−	-	-	−

Kidneys were isolated from 8–12-mo-old mice (either regular animals or bone marrow chimeras) of the indicated genotypes, processed, and analyzed for infiltration of leukocytes by flow cytometry, as described in Materials and methods. The absolute number of total leukocytes (CD45$^+$), B cells (CD19$^+$), myeloid cells (Mac-1$^+$), and T cells (TCRβ$^+$), and the percentage of activated effector T cells (TCRβ$^+$CD44^{high}CD62L$^-$) are reported as means ± SEM (n = 8–12). Statistical differences between *HFL*$^{-/-}$ or *lyn*$^{-/-}$ *IFNγ*$^{-/-}$ versus *lyn*$^{-/-}$ mice are reported. Similarly, statistical differences between *rag*$^{-/-}$-WT versus *lyn*$^{-/-}$*rag*$^{-/-}$-WT chimeras are reported. *, P < 0.05; **, P < 0.01; ***, P < 0.001. Histological analysis of renal disease as well as of Ig immune complex and C3 deposit immunofluorescent staining intensity was performed as described in Materials and methods. Data are representative of 10–20 mice for each genotype analyzed at end-point experiments.

cells. To achieve this, we crossed *lyn*$^{-/-}$ mice to *rag*$^{-/-}$ animals and used bone marrow from the CD45.2$^+$ *lyn*$^{-/-}$*rag*$^{-/-}$ mice or *rag*$^{-/-}$ mice (as controls), mixed with CD45.1$^+$ WT bone marrow (in a ratio of 75:25%) to reconstitute the hematopoietic system of lethally irradiated CD45.1$^+$ WT animals. WT control chimeras were generated by reconstituting lethally irradiated CD45.2$^+$ WT animals with CD45.1$^+$ WT bone marrow (Fig. S4 A). The *lyn*$^{-/-}$*rag*$^{-/-}$ and *rag*$^{-/-}$ mixed bone marrow chimeras (referred to as *lyn*$^{-/-}$*rag*$^{-/-}$-WT and *rag*$^{-/-}$-WT chimeras) both had modestly elevated serum BAFF levels at 2 mo after reconstitution because of mild lymphopenia caused by the 75% *rag*$^{-/-}$ bone marrow cells; however, only the *lyn*$^{-/-}$*rag*$^{-/-}$-WT chimeras showed a progressive increase in BAFF with age (Fig. 4 A). Similarly, starting between 3 and 4 mo of age, *lyn*$^{-/-}$*rag*$^{-/-}$-WT chimeras progressively developed splenomegaly and myeloproliferation (Fig. 4, B and C, left; and Fig. S4 B) that, by 10 mo of age, were indistinguishable from unmanipulated *lyn*$^{-/-}$ mice. The WT B cells present in the *lyn*$^{-/-}$*rag*$^{-/-}$-WT chimeras developed a hyperactivated phenotype with increased numbers of CD69$^+$ B cells and plasma cells (Fig. 4 C, right) that produced high levels of autoreactive IgM antibodies (Fig. 4 D). Both *lyn*$^{-/-}$*rag*$^{-/-}$-WT and *rag*$^{-/-}$-WT chimeras developed increased anti-dsDNA (and anti-RNA; not depicted) IgM autoantibodies and total IgM compared with control WT chimeras, with *lyn*$^{-/-}$*rag*$^{-/-}$-WT chimeras being more severe (Fig. S4 C). Furthermore, 50–60% of *lyn*$^{-/-}$*rag*$^{-/-}$-WT chimeras (but none of the *rag*$^{-/-}$-WT or WT chimeras) had serum ANA autoantibodies that showed a mild speckled staining pattern indicative of the presence of low levels of anti-RNA IgG antibodies (Fig. S4 D). The WT T cells in the *lyn*$^{-/-}$*rag*$^{-/-}$-WT chimeras also became activated with a significant expansion of CD69$^+$, effector, or IFN-γ–secreting cells, reaching levels similar to unmanipulated *lyn*$^{-/-}$ mice (Fig. 4 C, right). Aged *lyn*$^{-/-}$*rag*$^{-/-}$ chimeras also developed obvious evidence of kidney inflammation with increased interstitial nephritis and cellular infiltration mainly by Mac-1$^+$ myeloid cells and activated T cells (Fig. 4 E, Fig. S4 E, and Table I). Consistent with the serological data, immunofluorescent staining revealed increased IgM deposits in the glomeruli of *lyn*$^{-/-}$*rag*$^{-/-}$-WT chimeras (Fig. S4 F and Table I). Interestingly, probably because of a lack of glomerular IgG and C3 deposits, *lyn*$^{-/-}$*rag*$^{-/-}$-WT chimeras manifested a lower level of glomerulonephritis compared with unmanipulated *lyn*$^{-/-}$ mice. These data demonstrate that myeloid-restricted deletion of Lyn is sufficient to induce elevated serum levels of BAFF, myeloproliferation, B cell activation, T cell activation with increased IFN-γ production, and autoimmune nephritis.

IFN-γ deficiency reduces BAFF serum levels and ameliorates autoimmunity in *lyn*$^{-/-}$ mice

The described observations suggest a pathological interrelationship between BAFF release by myeloid cells and IFN-γ production by T cells that may contribute to the development of nephritis in *lyn*$^{-/-}$ mice. To further explore this, we generated animals deficient for both Lyn and IFN-γ (*lyn*$^{-/-}$ *IFNγ*$^{-/-}$). We found that many of the Lyn deficiency–induced phenotypes were attenuated in *lyn*$^{-/-}$*IFNγ*$^{-/-}$ mice. Serum BAFF levels were strongly reduced in aged *lyn*$^{-/-}$ *IFNγ*$^{-/-}$ mice, as was BAFF mRNA expression in splenic myeloid cells (or total spleen cells) compared with single mutant *lyn*$^{-/-}$ mice (Fig. 5, A and B, left). Importantly, IFN-γ

deficiency also dramatically reduced both the myeloproliferation and T cell activation present in *lyn*$^{-/-}$ mice (Fig. 5, C and D; and Fig. S5 A). On the other hand, the phenotype and accumulation of activated B lymphocytes and plasma cells (in the setting of overall B cell lymphopenia) was mostly unchanged in *lyn*$^{-/-}$*IFNγ*$^{-/-}$ compared with *lyn*$^{-/-}$ mice (Fig. 5 D and Fig. S5 B). Although IFN-γ deficiency reduced the level of autoreactive (mainly IgG2a/c) but not total IgG antibodies in *lyn*$^{-/-}$ mice, the *lyn*$^{-/-}$*IFNγ*$^{-/-}$ animals still overproduced total and autoreactive IgM autoantibodies (Fig. S5 C). The important role of IFN-γ in the production of IgG2a/c pathogenic antibodies in *lyn*$^{-/-}$ mice is in agreement with other mouse models of lupus-like disease (Balomenos et al., 1998; Theofilopoulos et al., 2001). Sera from *lyn*$^{-/-}$*IFNγ*$^{-/-}$ mice also showed a dramatic reduction of ANA staining intensity (Fig. S5 D). The *lyn*$^{-/-}$*IFNγ*$^{-/-}$ animals manifested a remarkable improvement in the kidney pathology (both interstitial and glomerulonephritis) compared with *lyn*$^{-/-}$ mice, with strongly reduced infiltration of CD45^{+} leukocytes (mainly Mac-1^{+} myeloid cells and activated T cells) and no formation of IgG immune complex or C3 deposits (Fig. 5 E; Fig. S5, E and F; and Table I). Finally, in a similar fashion to *HFL*$^{-/-}$ mice, BAFF mRNA expression was also strongly reduced in the kidneys of *lyn*$^{-/-}$*IFNγ*$^{-/-}$ mice (Fig. 5 B,

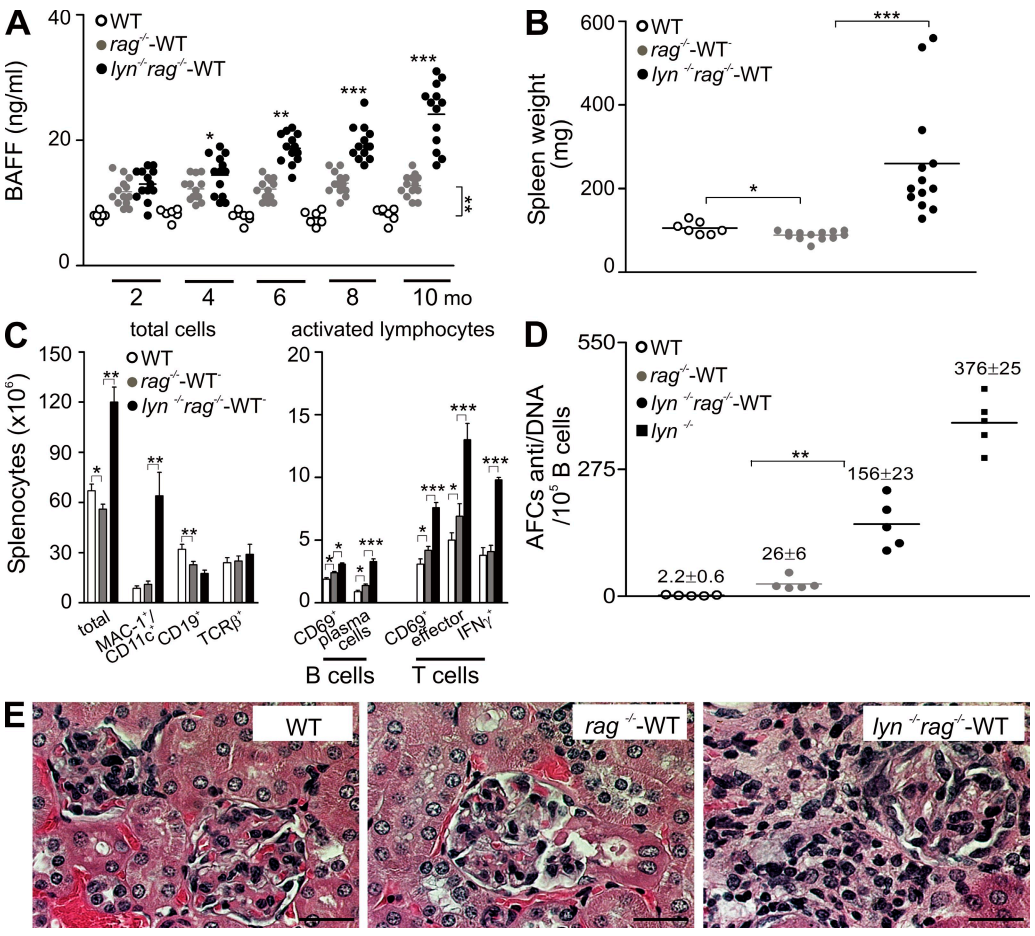

Figure 4. Myeloid-specific Lyn deficiency induces elevated BAFF serum levels and autoimmunity. WT, *rag*$^{-/-}$-WT, and *lyn*$^{-/-}$*rag*$^{-/-}$-WT chimeras were generated as described in Materials and methods. (A) BAFF serum levels in WT, *rag*$^{-/-}$-WT, and *lyn*$^{-/-}$*rag*$^{-/-}$-WT chimeras, assessed by ELISA. Each symbol represents the BAFF serum level of an individual mouse. Horizontal bars represent means. Data are pooled from three independent kinetic experiments. (B) Each symbol represents the weight of an individual spleen from 10-mo-old WT, *rag*$^{-/-}$-WT, and *lyn*$^{-/-}$*rag*$^{-/-}$-WT chimeras. Horizontal bars represent means. Data are pooled from three independent end-point experiments (n = 6–14). (C) Single-cell suspensions of spleens from 8–10-mo-old WT, *rag*$^{-/-}$-WT, and *lyn*$^{-/-}$*rag*$^{-/-}$-WT chimeras were counted and stained for FACS analysis. (left) The absolute number of total cells and (right) the absolute number of activated lymphocytes, calculated as described for Fig. 3. Data are expressed as means ± SEM (n = 10 mice per group). Statistical differences of *lyn*$^{-/-}$*rag*$^{-/-}$-WT versus *rag*$^{-/-}$-WT chimeras or *rag*$^{-/-}$-WT versus WT chimeras are reported. Data are pooled from three independent end-point experiments. (D) A single-cell suspension of spleens was prepared and the frequencies of IgM-secreting AFCs specific to DNA were assessed by ELISPOT in 8–10-mo-old WT, *rag*$^{-/-}$-WT, or *lyn*$^{-/-}$*rag*$^{-/-}$-WT chimeras or *lyn*$^{-/-}$ mice. Statistical differences of *lyn*$^{-/-}$*rag*$^{-/-}$-WT versus *rag*$^{-/-}$-WT chimeras are reported. Horizontal bars represent means. Data are representative of five independent experiments. *, $P < 0.05$; **, $P < 0.01$; ***, $P < 0.001$. (E) Representative H&E staining of kidneys from 8–10-mo-old WT, *rag*$^{-/-}$-WT, and *lyn*$^{-/-}$*rag*$^{-/-}$-WT chimeras. Bars, 100 µm. Data are representative of >20 mice for each genotype analyzed at end-point experiments.

right). These results indicate that IFN-γ contributes to myeloproliferation, BAFF overproduction, and T cell activation in this model.

To further validate the interrelationship between BAFF release by myeloid cells and IFN-γ production by T cells, we generated animals lacking Lyn in the myeloid cell compartment and IFN-γ in the lymphoid compartment by creating $lyn^{-/-}rag^{-/-}$ chimeras mixed with IFN-γ–deficient bone marrow cells. These mixed chimeric animals did not show myeloproliferation, had lower levels of BAFF, reduced T cell activation, and reduced nephritis (Fig. S6). In contrast to the $lyn^{-/-}IFN\gamma^{-/-}$ mice, which showed persistent B cell activation and IgM autoantibody production because of a deficiency of Lyn in B cells, activation of the WT B cells in the $lyn^{-/-}rag^{-/-}$-$IFN\gamma^{-/-}$ chimeras was lower than in the $lyn^{-/-}rag^{-/-}$ chimeras. These observations suggest that lymphocytes (i.e., T or possibly NKT cells), not NK or myeloid cells, are the primary source of IFN-γ necessary to drive myeloproliferation, BAFF overproduction, and nephritis in $lyn^{-/-}$ mice (or in animals lacking Lyn in the myeloid compartment alone).

Because genetic deletion of IFN-γ in lymphocytes blocked disease development, we reasoned that treatment with recombinant IFN-γ should accelerate the process. Indeed, both $lyn^{-/-}$ mice and $lyn^{-/-}rag^{-/-}$-WT chimeras developed severe myeloproliferation, dramatically elevated BAFF production, T cell activation, and nephritis after 3 mo of treatment with rIFN-γ (unpublished data). Autoantibody production was unaffected and rIFN-γ treatment had no effect on WT

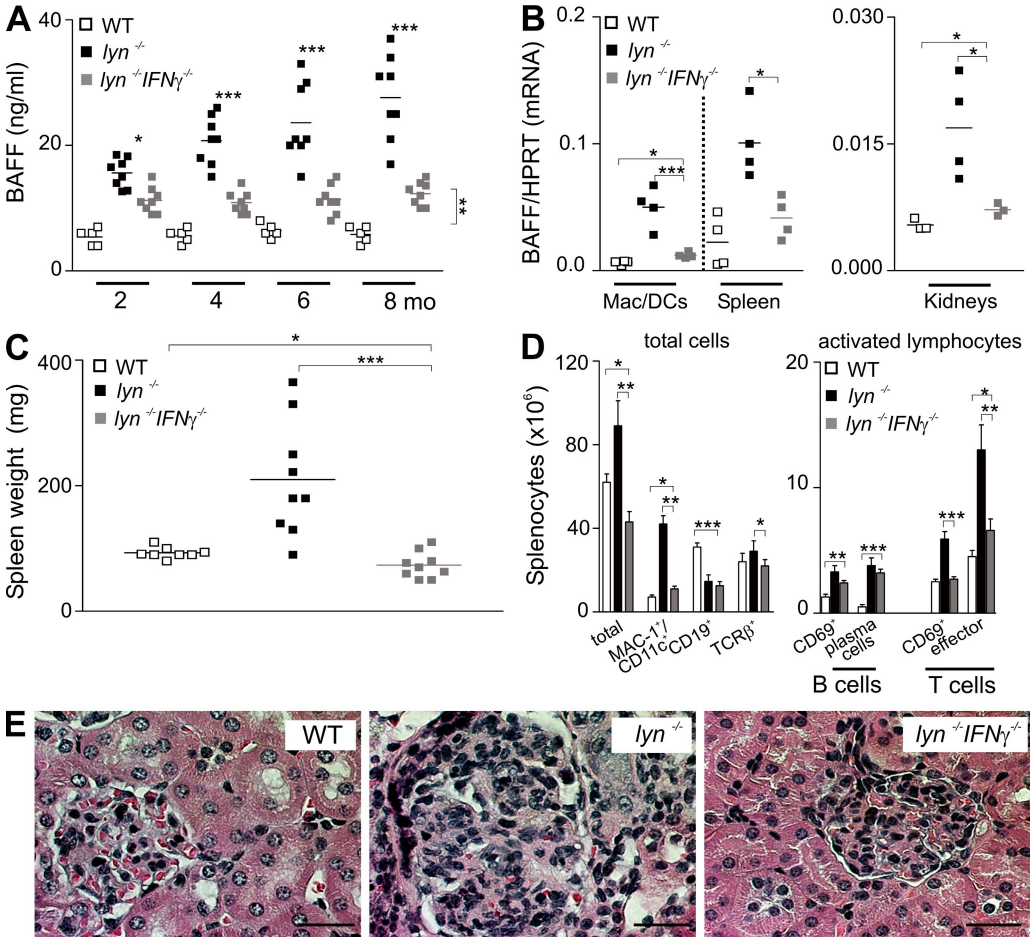

Figure 5. IFN-γ deficiency reduces BAFF serum levels, blocks splenomegaly, and improves autoimmunity in $lyn^{-/-}$ mice. (A) BAFF serum levels in WT, $lyn^{-/-}$, and $lyn^{-/-}IFN\gamma^{-/-}$ mice, assessed by ELISA. Each symbol represents the BAFF serum level of an individual mouse. Data are pooled from two independent kinetic experiments (n = 5–8). (B) BAFF mRNA expression in sorted splenic macrophages and DCs ($F4/80^+CD11c^+$) and total spleens (left) or total kidneys (right) from 6–10-mo-old WT, $lyn^{-/-}$, or $lyn^{-/-}IFN\gamma^{-/-}$ mice. Data are representative of one end-point experiment (n = 4). (C) Each symbol represents the weight of an individual spleen from 8–10-mo-old WT, $lyn^{-/-}$, or $lyn^{-/-}IFN\gamma^{-/-}$ mice. Data are pooled from two independent end-point experiments (n = 8–9). Horizontal bars in A–C represent means. (D) Single-cell suspensions of spleens from 8–10-mo-old WT, $lyn^{-/-}$, or $lyn^{-/-}IFN\gamma^{-/-}$ mice were counted and stained for FACS analysis. (left) The absolute number of total cells and (right) the absolute number of activated lymphocytes, calculated as described for Fig. 3. Data are expressed as means ± SEM (n = 9 mice per group). Statistical differences of $lyn^{-/-}IFN\gamma^{-/-}$ versus $lyn^{-/-}$ mice or $lyn^{-/-}IFN\gamma^{-/-}$ versus WT mice are reported. Data are pooled from two independent end-point experiments. *, $P < 0.05$; **, $P < 0.01$; ***, $P < 0.001$. (E) Representative H&E staining of kidney sections from 8–10-mo-old WT, $lyn^{-/-}$, or $lyn^{-/-}IFN\gamma^{-/-}$ mice. Bars, 100 µm. Data are representative of 10–15 mice for each genotype analyzed at end-point experiments.

mice. Thus, in response to elevated IFN-γ, the hyperreactive *lyn*$^{-/-}$ myeloid cells released large amounts of BAFF and induced an accelerated inflammatory/autoimmune process.

Reduction of BAFF activity ameliorates the development of autoimmunity in *lyn*$^{-/-}$ mice

Our observations suggest that the dysregulated myeloproliferation and BAFF production caused by Lyn deficiency might lead to increased T cell activation and IFN-γ release that, in turn, could feed back on the myeloid compartment to increase hyperreactivity. To directly test the role of BAFF in this pathogenic loop, we used a neutralizing anti-BAFF mAb to reduce BAFF activity. In line with observations reported by others (Kalled, 2005; Mackay and Schneider, 2009), we found that the administration of high doses of neutralizing anti-BAFF mAb (>100 µg/20 g mouse) led to complete and prolonged mature B cell depletion, as well as strong reduction in T cell activation, myeloproliferation, and nephritis in *lyn*$^{-/-}$ mice (unpublished data). Because it is well known that B cell depletion in autoimmune models leads to diminution of T cell activation and disease amelioration, these results were expected (Shlomchik et al., 2001; Yanaba et al., 2008; Dörner et al., 2009). However, to better understand the pathological role of BAFF in Lyn-deficient autoimmunity, we sought to only partially reduce BAFF levels in *lyn*$^{-/-}$ mice without producing significant B cell depletion. We hypothesized that a reduction in BAFF levels would reduce the myeloproliferation, T cell activation, and IFN-γ overproduction that characterize the *lyn*$^{-/-}$ autoimmune phenotype. To partially reduce BAFF activity, we established an anti-BAFF dosing regimen using small amounts of anti-BAFF mAb administered every other day for several months (see Materials and methods). We did this experiment in both 6–8-wk-old mice, before disease onset, and 6–7-mo-old mice with active disease.

In young *lyn*$^{-/-}$ mice (before the onset of myeloproliferation and significant B or T cell activation) treated every other day for 5 mo (long-term treatment), the number and percentage of B cells was reduced by ∼50%, although the distribution of remaining B cell subtypes was similar to untreated *lyn*$^{-/-}$ mice (Fig. 6, A and B, left; and Fig. S7 A, left). This 5-mo anti-BAFF mAb treatment partially reversed the hyperreactive phenotype of *lyn*$^{-/-}$ B cells (Fig. 6, A and B, right; and Fig. S7 A, right). The serum level of autoreactive IgG antibodies (but not IgM) was significantly reduced, whereas total Ig levels remained the same (Fig. 6 C and Fig. S7 B). Besides these partial effects on B cell activation, the low-dose anti-BAFF treatment dramatically reduced both myeloproliferation and T cell activation in *lyn*$^{-/-}$ mice (Fig. 6, A, B, and D). Both the number and percentage of activated and IFN-γ–producing T cells (of both the CD4 and CD8 subtypes) was strongly reduced in 5-mo anti-BAFF mAb–treated *lyn*$^{-/-}$ mice as compared with the isotype control–treated animals (Fig. 6, A and B, right). As a result, serum IFN-γ in the treated young *lyn*$^{-/-}$ mice was reduced to almost undetectable levels by the anti-BAFF mAb treatment (Fig. S7 C). Finally, the 5-mo anti-BAFF mAb treatment induced a clear improvement of nephritis in *lyn*$^{-/-}$ mice (both interstitial and glomerulonephritis) by reducing IgG (but not IgM) immune complex and C3 deposits, as well as the infiltration of myeloid cells and activated T cells (Fig. 6 E; Fig. S7, D and E; and Table II).

In the 6–7-mo-old *lyn*$^{-/-}$ mice, we performed a 2-mo anti-BAFF treatment protocol (short-term treatment). At this stage of life, *lyn*$^{-/-}$ mice have large numbers of activated B cells, plasma cells, extreme myeloproliferation, very high levels of activated T cells (with high IFN-γ production), and established nephritis. After short-term anti-BAFF mAb treatment, the myeloproliferation, T cell activation, and IFN-γ production were strongly reduced in *lyn*$^{-/-}$ mice, whereas the number of activated B cells as well as autoantibody and total Ig production was minimally affected (Fig. 6, F–I; and Fig. S8, A and B). The latter phenomenon was likely caused by reduced BAFF receptor expression in fully activated B cells and by the shift in dependency of activated memory or plasma cells on other survival factors besides BAFF (Ng et al., 2005; Ramanujam et al., 2006; Ettinger et al., 2007; Scholz et al., 2008). This short-term treatment of older *lyn*$^{-/-}$ mice also partially reversed the extent of nephritis by improving mainly the interstitial nephritis and to a lesser extent the glomerulonephritis (Fig. 6 J and Fig. S8 C). These data indicate that even in older *lyn*$^{-/-}$ mice with well-established disease, the anti-BAFF treatment could reduce T cell activation, IFN-γ production, and subsequent

Table II. Reduction of BAFF activity reduces the infiltration of leukocytes into the kidneys of *lyn*$^{-/-}$ mice

Treatment	*lyn*$^{-/-}$	*lyn*$^{-/-}$ + anti-BAFF antibody
CD45^{+} (×10^{5})	18.5 ± 4	9.8 ± 1.4*
CD45^{+}CD19^{+} (×10^{5})	0.9 ± 0.2	0.15 ± 0.05**
CD45^{+}Mac-1^{+} (×10^{5})	12.3 ± 4	5.1 ± 0.6*
CD45^{+}TCRβ^{+} (×10^{5})	5.2 ± 0.8	4.5 ± 0.5
CD45^{+}TCRβ^{+}CD44^{high}CD62L^{-} (%)	77 ± 2	52 ± 5***
Histological score		
Glomerulonephritis	2.2 ± 0.3	1.1 ± 0.21**
Interstitial nephritis	2 ± 0.2	0.6 ± 0.1***
Immunofluorescence staining intensity		
IgM deposit score	+++	+++
IgG deposit score	++	+/−
C3 deposit score	+++	+/−

Young (2-mo-old) *lyn*$^{-/-}$ mice were treated with neutralizing anti-BAFF mAb or irrelevant isotype control mAb for 5 mo (long-term treatment), as described in Materials and methods. Mice were sacrificed, and kidneys were isolated, processed, and analyzed for infiltration of leukocytes by flow cytometry, as described in Materials and methods. The absolute number of total leukocytes (CD45^{+}), B cells (CD19^{+}), myeloid cells (Mac-1^{+}), and T cells (TCRβ^{+}), and the percentage of activated effector T cells (TCRβ^{+}CD44^{high}CD62L^{-}) are reported as means ± SEM (n = 7–10). *, P < 0.05; **, P < 0.01; ***, P < 0.001. Histological analysis of renal disease as well as of Ig immune complex and C3 deposit immunofluorescent staining intensity was performed as described in Materials and methods. Data are representative of 12 mice for each genotype analyzed at end-point experiments.

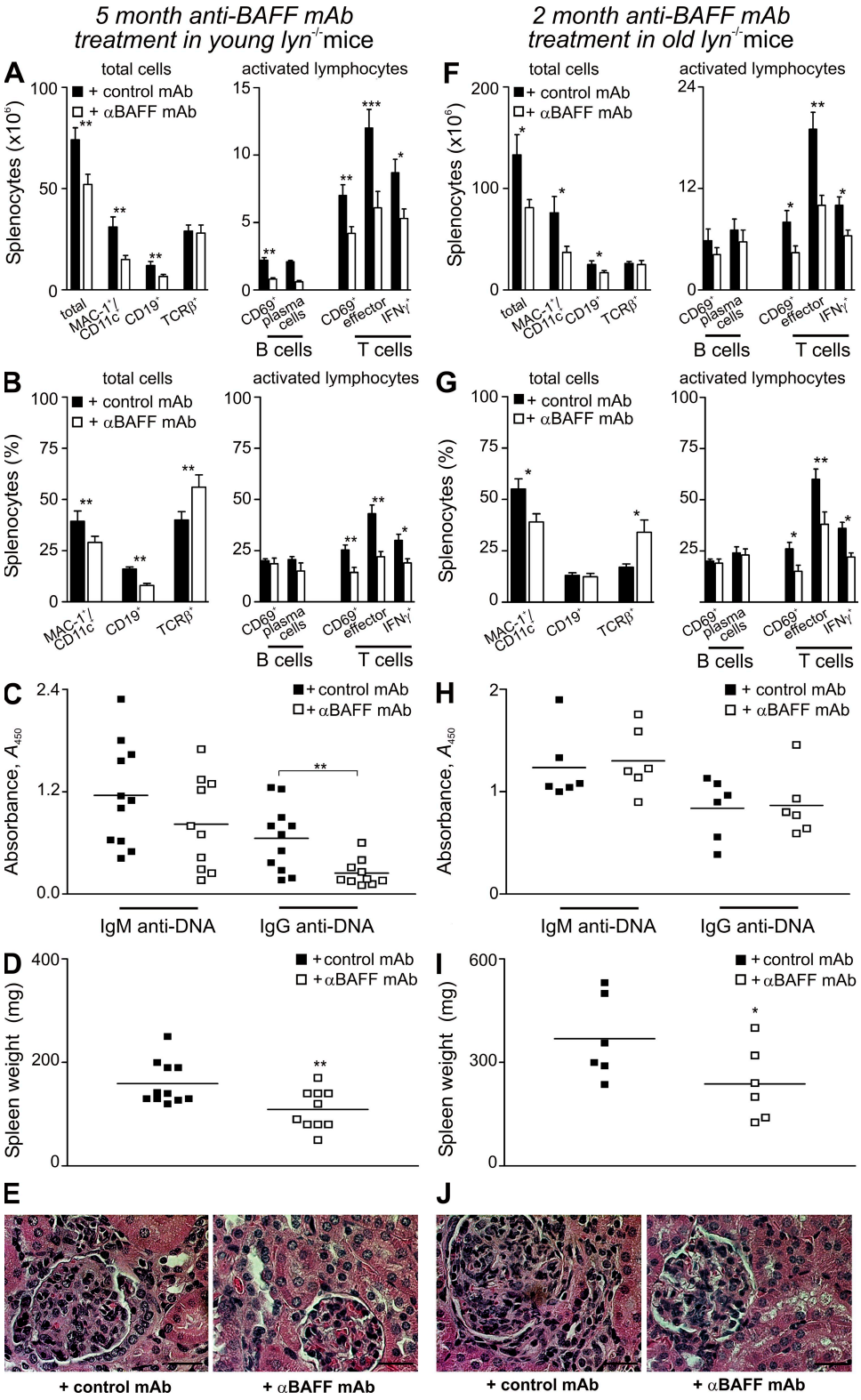

Figure 6. Reduction of BAFF activity ameliorates autoimmune abnormalities in *lyn*$^{-/-}$ mice. (A–J) Young (2-mo-old) *lyn*$^{-/-}$ mice were treated for 5 mo (long-term treatment; A–E) or old (6–7-mo-old) *lyn*$^{-/-}$ mice were treated for 2 mo (short-term treatment; F–J) with neutralizing anti-BAFF mAb or irrelevant isotype control mAb, as described in Materials and methods. (A, B, F, and G) Single-cell suspensions of spleens from *lyn*$^{-/-}$ mice after 5 mo (A and B) or 2 mo (F and G) of treatment with anti-BAFF mAb were counted and stained for FACS analysis. (left) The absolute number (A and F) and percentage (B and G) of total cells and (right) the absolute number (A and F) and percentage (B and G) of activated lymphocytes, calculated as described for Fig. 3.

myeloid cell hyperreactivity without dramatically affecting B cell numbers or activation.

BAFF supports T cell activation and IFN-γ production in vivo

To directly test whether the high BAFF in *lyn*$^{-/-}$ mice can directly contribute to the activation of T cells in vivo independently from the effect of this cytokine on B cell activation, we performed adoptive transfer of WT or BAFF receptor–deficient (*BAFF-R*$^{-/-}$) T cells into 6–7-mo-old *lyn*$^{-/-}$ mice (or WT mice as controls). To perform these experiments, we injected a 1:1 ratio mixture of freshly isolated naive splenic WT and *BAFF-R*$^{-/-}$ T cells, which could be distinguished by differential expression of the congenic marker CD45.1/2. 15 d after the transfer, we observed no significant changes in activation or IFN-γ production of either WT or *BAFF-R*$^{-/-}$ donor T cells when transferred in WT host mice (Fig. 7 A). On the other hand, although donor WT T cells transferred in *lyn*$^{-/-}$ mice reached levels of activation that were indistinguishable from endogenous host *lyn*$^{-/-}$ T cells, the *BAFF-R*$^{-/-}$ T cells showed much lower levels of CD44, higher expression of CD62L, and reduced IFN-γ expression (Fig. 7, A and B). The reduced response in vivo of *BAFF-R*$^{-/-}$ T cells is not caused by general functional impairment because *BAFF-R*$^{-/-}$ T cells develop normally and respond normally to anti-CD3/anti-CD28 stimulation in vitro (Ng et al., 2004; Mackay and Leung, 2006). These data indicate that *BAFF-R*$^{-/-}$ T cells show reduced activation and IFN-γ production when transferred into *lyn*$^{-/-}$ mice, suggesting that the overproduction of BAFF in these animals is a direct contributor to enhanced T cell activation.

DISCUSSION

lyn$^{-/-}$ mice develop a progressive lupus-like autoimmunity that, to date, has been mainly attributed to B cell hyperactivation and abnormalities in B cell tolerance mechanisms (Hibbs et al., 1995; Nishizumi et al., 1995; Chan et al., 1997; Xu et al., 2005). Our results demonstrate that the myeloid compartment plays a crucial role for development of autoimmunity in *lyn*$^{-/-}$ mice. We propose that the deregulation of myeloid cell responses in *lyn*$^{-/-}$ mice leads to overproduction of BAFF, which acts on B cells as expected but also activates T cells, leading to increased IFN-γ release, which further increases myeloid cell hyperactivity. The reciprocal production of BAFF and IFN-γ establishes a self-sustaining inflammatory loop that is crucial for progression of autoimmunity caused by Lyn deficiency (Fig. 8). This inflammatory loop also develops in mice having only a Lyn-deficient myeloid compartment and a WT lymphocyte compartment, which strengthens the argument that deregulation of myeloid cell function is a key pathogenic feature in this model. Blocking this inflammatory loop by reducing myeloid cell hyperreactivity (using *HFL*$^{-/-}$ mice), lowering BAFF (using mAb treatment), or removing IFN-γ (genetically) prevented nephritis in *lyn*$^{-/-}$ animals. Overall, our observations demonstrate that overproduction of BAFF by innate immune cells in a lupus-like disease setting can directly increase T cell activation and IFN-γ production by these cells, suggesting that this is an additional pathological role of BAFF in this disease that may have been underestimated.

Although our observations suggest the establishment of an inflammatory loop between myeloid cells and T cells that exacerbates autoimmunity in *lyn*$^{-/-}$ mice, it still remains unclear what initiates the process. There are several potential mechanisms for initiation of the inflammation/autoimmunity in *lyn*$^{-/-}$ mice. First, the intrinsic effects of Lyn deletion on B cell tolerance thresholds leads to a degree of B cell activation, autoantibody production, and tissue deposition of immune complexes to which T cells and *lyn*$^{-/-}$ myeloid cells could then hyperrespond. Second, the relative B cell lymphopenia and resultant elevated serum BAFF in young *lyn*$^{-/-}$ mice may be adequate to promote increased B cell autoimmune responses (Schneider, 2005; Sarantopoulos et al., 2007). The third possible mechanism may involve myeloid cell hyperactivity toward Toll-like receptor (TLR) agonists (present in commensal flora or from environmental sources). Silver et al. (2007) have recently demonstrated that loss of TLR signaling through MyD88 deficiency prevents development of autoimmunity in *lyn*$^{-/-}$ mice, suggesting that chronic stimulation of TLRs by endogenous flora may also contribute to the disease. Of course, all three of these mechanisms may contribute together toward establishment of the inflammatory loop. However, intrinsic defects in B cells alone are not sufficient to establish the full autoimmune phenotype in *lyn*$^{-/-}$ mice, because both the *HFL*$^{-/-}$ and *lyn*$^{-/-}$*IFNγ*$^{-/-}$ animals manifest much of the B cell hyperactivity caused by the lack of Lyn, yet neither of these strains develop the inflammatory/autoimmune nephritis. These data are in agreement with several reports in the literature revealing that autoantibody production alone is not sufficient to produce end-organ damage (Chan et al., 1999; Bagavant and Fu, 2005; Ramanujam and Davidson, 2008). Furthermore, in other mouse lupus models, BAFF blockade has been shown to decrease renal injury and inflammation without inducing a strong reduction of immune complex deposition in the kidney, suggesting that a direct pathogenic role of BAFF in regulating the inflammatory damage in the target organ is

Data are expressed as means ± SEM (n = 10–11 mice per group in A and B or 5–6 mice per group in F and G). Date are representative of two independent end-point experiments. (C and H) Effect of 5 mo (C) or 2 mo (H) of anti-BAFF mAb treatment on the levels of IgM and IgG specific to DNA in *lyn*$^{-/-}$ mice, assessed by ELISA. Data are representative of two independent end-point experiments (n = 10–12). (D and I) Effect of 5 mo (D) or 2 mo (I) of anti-BAFF mAb treatment on the development of splenomegaly in *lyn*$^{-/-}$ mice. Data are representative of two independent end-point experiments (n = 10–12). *, $P < 0.05$; **, $P < 0.01$; ***, $P < 0.001$. Horizontal bars in C, D, H, and I represent means. (E and J) Representative H&E staining of kidneys from *lyn*$^{-/-}$ mice after 5 mo (E) or 2 mo (J) of treatment with anti-BAFF mAb. Bars, 100 µm. Data are representative of 12–16 mice for each treatment analyzed at end-point experiments.

independent from the induction of pathogenic IgG autoantibodies (Stohl et al., 2005; Ramanujam et al., 2006; Ramanujam and Davidson, 2008; Moisini and Davidson, 2009). Several studies have suggested that IFN-γ plays an important role in the progression of nephritis (Theofilopoulos et al., 2001).

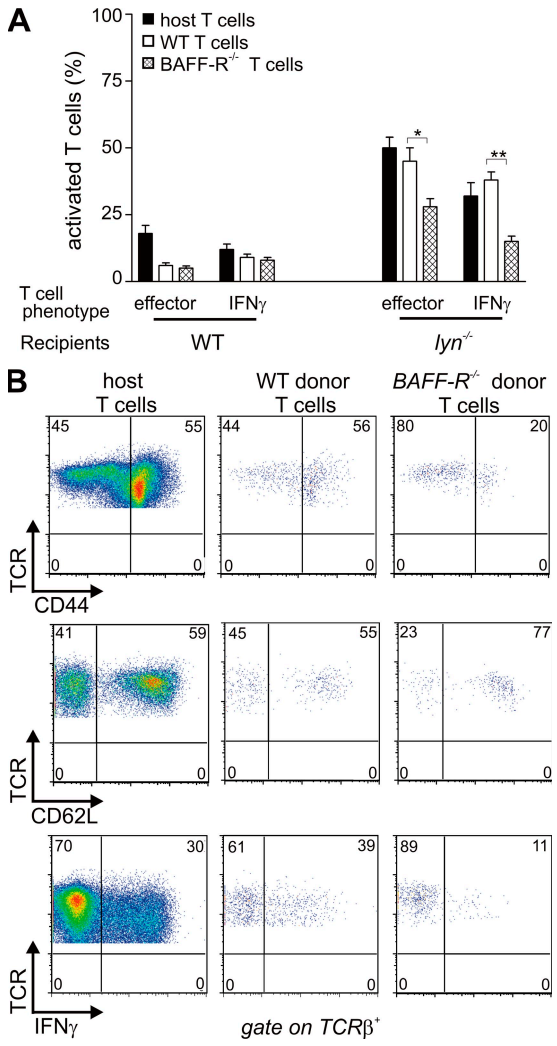

Figure 7. *BAFF-R*$^{-/-}$ T cells fail to become activated when transferred to *lyn*$^{-/-}$ recipients. (A) Resting T cells isolated from single-cell suspensions of WT (CD45.1/2 het) or *BAFF-R*$^{-/-}$ (CD45.2) mouse spleens and lymph nodes were mixed in a 1:1 ratio and injected i.v. into 6–7-mo-old WT or *lyn*$^{-/-}$ mice (CD45.1). 15 d after transfer, the levels of T cell activation and IFN-γ production in host and donor T cells were analyzed by taking advantage of the differential expression of the CD45.1/2 markers by flow cytometry, as described in Materials and methods. The percentage of activated/effector (CD44^{high}CD62L^{-}) or IFN-γ–producing host and donor (WT or *BAFF-R*$^{-/-}$) T cells detected in the spleens of host WT or *lyn*$^{-/-}$ mice 15 d after adoptive transfer are reported. Data are expressed as means ± SEM (n = 7 mice per group). Data are pooled from two independent experiments. *, $P < 0.05$; **, $P < 0.01$. (B) Representative FACS plots of CD44 (top), CD62L (middle), or IFN-γ (bottom) expression by host (left) and donor WT (middle) or *BAFF-R*$^{-/-}$ (right) T (TCRβ^{+}) cells detected in the spleens of host *lyn*$^{-/-}$ mice 15 d after adoptive transfer are reported. Data are representative of seven mice for each condition.

The interplay between BAFF production by myeloid cells and IFN-γ production by T cells could be a key pathogenic mechanism contributing to many aspects of lupus-like disorders.

Although we have focused on overproduction of BAFF as playing a central role in the development of autoimmunity in *lyn*$^{-/-}$ mice, it is very likely that other cytokines contribute to the disease process as well. Indeed, we have observed elevated levels of IL-6, GM-CSF, and M-CSF in these mice, and they too may be involved in the inflammatory/autoimmune loop (unpublished data). IL-6 has been found to be involved in the autoimmune process in several mouse model of lupus (Liang et al., 2006; Maeda et al., 2009; Cash et al., 2010) and, more recently, in *lyn*$^{-/-}$ mice (Tsantikos et al., 2009). Furthermore, a pathological role for myeloid cell–specific CSFs, such as M-CSF and GM-CSF, in inflammation and autoimmunity has been suggested (Hamilton, 2008). On the other hand, both genetic deletion of IFN-γ and reduction of BAFF activity dramatically lowered the serum levels of these proinflammatory cytokines (unpublished data). Hence, although BAFF and IFN-γ are probably not the only cytokines involved, they are necessary for disease progression in *lyn*$^{-/-}$ mice.

The anti-BAFF mAb treatment experiments provide important insights into the relationship between BAFF, T cell activation, and IFN-γ production. Although the partial (in young *lyn*$^{-/-}$ mice) or minimal (in older *lyn*$^{-/-}$ mice) reduction in activated B cells and autoantibody production achieved by administration of low-dose anti-BAFF mAb was expected, the reduction in T cell activation, IFN-γ production, and myeloproliferation in both young and old *lyn*$^{-/-}$ mice was unexpected. We have also performed low-dose anti-BAFF treatment of *lyn*$^{-/-}$*rag*$^{-/-}$-WT chimeras lacking Lyn in myeloid cells only, and have seen similar effects on T cell activation and myeloproliferation (unpublished data). Our proposal that BAFF plays an important role in autoimmune disease in part through its effect on T cells is supported by in vitro findings demonstrating that BAFF acts as a co-stimulatory molecule to enhance T cell activation and differentiation into IFN-γ–secreting cells, mainly through the interaction with BAFF-R (Huard et al., 2001; Mackay and Leung, 2006). BAFF effects on T cells via BAFF-R have also been shown in vivo in a transplantation setting (Ye et al., 2004). Similarly, our observation that WT T cells become activated and secrete IFN-γ when adoptively transferred into *lyn*$^{-/-}$ mice, whereas *BAFF-R*$^{-/-}$ T cells show weak responses, supports the notion that BAFF is acting directly on T cells. The low level of activation still present in *BAFF-R*$^{-/-}$ T cells transferred in *lyn*$^{-/-}$ mice is likely caused by other proinflammatory cytokines that sustain/induce T cell activation (such as TNF and IL-6), which are present in *lyn*$^{-/-}$ mice at a late stage of disease.

Collectively, our data indicate that dysregulated BAFF production by myeloid cells in response to activated T cell–derived IFN-γ establishes an inflammatory loop that is critical for the progression of autoimmunity in *lyn*$^{-/-}$ mice and, potentially, to autoimmune disorders in general (Fig. 8). In human lupus patients, an elevated number of IFN-γ–producing effector T cells and BAFF-producing monocytes has been

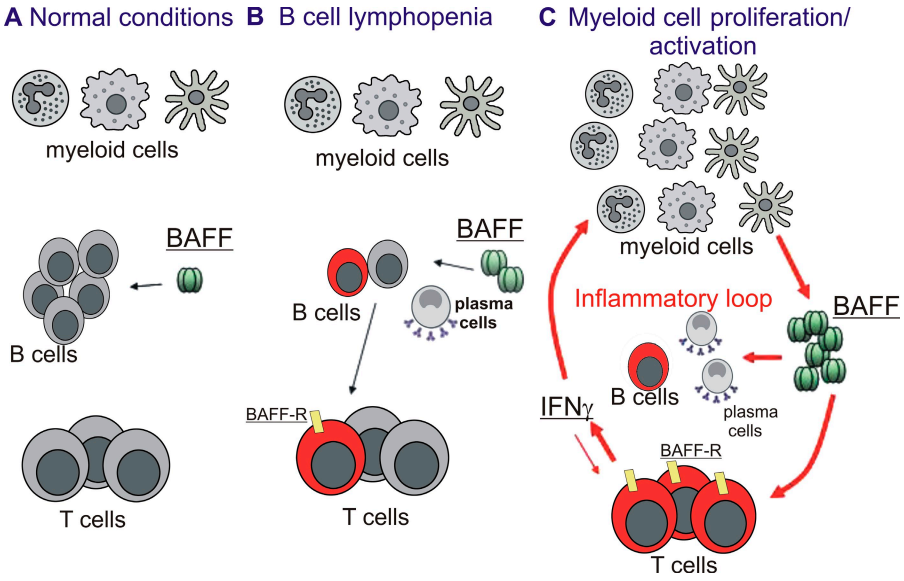

Figure 8. Proposed model to explain the role of BAFF, IFN-γ, and myeloid cells in Lyn-deficient autoimmunity. (A) Under normal conditions BAFF is produced in a fixed amount from stromal cells, thus regulating the size and the maturation status of the B cell compartment. (B) During B cell lymphopenia, BAFF serum levels rise, and the amount of BAFF available per B cell increases. In the Lyn-deficient model, the elevated serum BAFF caused by the B lymphopenia as well as the intrinsic hyperactivity of *lyn*$^{-/-}$ B cells contribute to increased B cell responses, leading to autoantibody production. This initial inflammatory insult is probably sufficient to partially activate T cells (which at this point can begin to express BAFF-R) and *lyn*$^{-/-}$ myeloid cells. (C) In more severe inflammatory conditions and/or during myeloid cell activation/proliferation, BAFF production dramatically increases, directly affecting both B cell and T cell activation, leading to differentiation of the latter cells into IFN-γ–producing T cells. IFN-γ, in a positive feedback loop, sustains more myeloid cell activation/proliferation and BAFF production, which in turn further amplifies the lymphocyte activation leading to autoimmunity and organ damage.

reported (Harigai et al., 2008). In view of the well-described role of BAFF in autoimmune diseases and of the interest in developing therapeutics able to neutralize BAFF (Ding, 2008; Ramanujam and Davidson, 2008; Moisini and Davidson, 2009), our study uncovers an important new pathological mechanism through which BAFF contributes to late-stage autoimmune disease by promoting a pathological cross talk between innate and adaptive immunity.

MATERIALS AND METHODS

Mice

lyn$^{-/-}$ and *HFL*$^{-/-}$ mice were previously established and backcrossed onto the C57BL/6 (B6, carrying the CD45.2 allele) background for 15 generations (Meng and Lowell, 1997; Pereira and Lowell, 2003). *lyn*$^{-/-}$ mice on the B6 background but carrying the CD45.1 allele were generated by crossbreeding with congenic WT mice carrying the CD45.1 allele on the B6 background (Taconic). Age-matched WT B6 mice (carrying the CD45.2 allele) were purchased from Charles River. WT mice heterozygous for the expression of both the CD45.1 and CD45.2 allele (WT CD45.1/2 het) mice were generated by crossbreading B6 (CD45.2) mice with congenic mice carrying the CD45.1 allele on the B6 background. *IFNγ*$^{-/-}$, *rag*$^{-/-}$, and *BAFF-R*$^{-/-}$ mice on a B6 background were obtained from the Jackson Laboratory. *lyn*$^{-/-}$ *IFNγ*$^{-/-}$ and *lyn*$^{-/-}$*rag*$^{-/-}$ mice were generated by crossbreeding *lyn*$^{-/-}$ mice and *IFNγ*$^{-/-}$ or *rag*$^{-/-}$ mice, respectively. Bone marrow chimeras were generated by injecting lethally irradiated congenic recipients carrying the CD45.1 allele on the B6 background (8–12 wk old) with a pool of bone marrow cells containing 75% cells from *lyn*$^{-/-}$*rag*$^{-/-}$ mice (or *rag*$^{-/-}$ mice, used as controls) carrying the CD45.2 allele, mixed with 25% cells from congenic CD45.1 WT mice (6–8 wk old). Lethally irradiated CD45.2 B6 mice reconstituted with 100% congenic CD45.1^{+} WT cells were also generated as controls. By this experimental approach, we were able to generate chimeric mice with a high level of deletion (75%) of Lyn in the myeloid compartment, whereas the lymphoid compartment was 100% WT. Multiple ratios of the mixed *lyn*$^{-/-}$*rag*$^{-/-}$ (or *rag*$^{-/-}$)-WT bone morrow chimeras (50:50% or 25:75%, respectively) were also generated and tested, but throughout the paper only data regarding the 75:25% *lyn*$^{-/-}$*rag*$^{-/-}$ (or *rag*$^{-/-}$)-WT chimeras are reported because of the more severe phenotype. Mixed 75:25% *lyn*$^{-/-}$*rag*$^{-/-}$-*IFNγ*$^{-/-}$ bone marrow chimeras were also generated in selected experiments. Chimeras were analyzed starting from 2 mo of age and followed for up to 1 yr for evidence of disease (see Materials and methods). The repopulation of the leukocyte compartments and the percentage of CD45.2^{+} *lyn*$^{-/-}$ *rag*$^{-/-}$ or *rag*$^{-/-}$ myeloid cells versus the CD45.1^{+} WT myeloid/lymphoid cells were evaluated as described in Flow cytometry (FACS). All animals were kept in a specific pathogen–free facility at the University of California, San Francisco (UCSF) and used according to protocols approved by the UCSF Committee on Animal Research.

Cell isolation and culture

BMD neutrophils were isolated from B6 and *lyn*$^{-/-}$ mice, as described previously (Pereira and Lowell, 2003). Immediately after purification, cells were suspended at 10^6 cells/ml in RPMI 1640 medium supplemented with 10% (volume/volume) FBS (Invitrogen), 100 U/ml penicillin G, 100 µg/ml streptomycin, and 2 mM L-glutamine (all from UCSF) and incubated at 37°C in 5% CO_2 in the presence or absence of the stimuli indicated in the figures for 24 h. Cells were collected and spun at 350 *g* for 5 min, and the resulting supernatants were stored at less than or equal to −20°C. BMD macrophages and BMD DCs were prepared from B6 or *lyn*$^{-/-}$ mice, as described previously (Pereira and Lowell, 2003; Chu and Lowell, 2005). BMD macrophages were used at day 6 of culture, whereas BMD DCs were used between days 8 and 10 of culture. Cells were washed, suspended at 10^6 cells/ml in the appropriate complete media without growth factor, plated in 24-well tissue culture plates, and incubated at 37°C in 5% CO_2 in the presence or absence of the stimuli indicated in the figures for 24 or 48 h for RNA or supernatant preparations, respectively. Cells were collected and spun at 350 *g* for 5 min, and the resulting supernatants were stored at less than or equal to −20°C. Cell pellets were processed for RNA extractions as described in RNA extractions and Taqman… In selected experiments, BMD macrophage and BMD DC culture supernatant preparations were run in parallel with a proliferation assay by using the CellTiter 96 Aqueous One Solution Cell Proliferation Assay (Promega) according to the manufacturer's instructions. The following stimuli and recombinant mouse cytokines were used: 20 ng/ml GM-CSF, 100 ng/ml IL-10, 20 ng/ml TNF, and 100 ng/ml IL-4 (PeproTech); 100 U/ml IFN-γ and 500 U/ml mIFN-α (Thermo Fisher Scientific); 100 ng/ml M-CSF (R&D Systems); and 1 µM fMLP and 50 ng/ml PMA (Sigma-Aldrich). For splenic DC and macrophage isolation, single-cell

suspensions were prepared after digestion of spleens with 500 U/ml collagenase D (Roche) followed by staining with fluorescent protein allophycocyanin (APC)-conjugated anti-F4/80 and anti-CD11c antibodies performed as described in the following section. Cells were suspended in PBS containing 300 nM DAPI (Sigma-Aldrich), 2 mM EDTA, and 2% (volume/volume) FBS before sorting using a high-speed sorter (MoFlo; Dako). The isolated myeloid cells had a purity of >98%.

Flow cytometry (FACS)

Leukocytes from peripheral blood and single-cell suspensions from spleens depleted of red blood cells were counted and resuspended in PBS containing 2 mM EDTA and 2% (volume/volume) FBS (staining/washing buffer). Kidneys were prepared as previously described (Kaneko et al., 2006) and resuspended in staining/washing buffer. For flow cytometry, cells were incubated for 5–10 min with 0.5 μg/10^6 cell anti-CD16/CD32 (2.4G2; UCSF) plus 100 μg purified mouse Ig (Sigma-Aldrich) per 10^6 cells to block FcRs before staining with the following anti–mouse FITC-conjugated, APC-conjugated, PE-conjugated, or biotinylated specific antibodies: CD19 (clone 1D3), CD21/35 (7G6), CD23 (B3B4), CD69 (H1.2F3), CD138 (281-2), CD11c (HL3), CD11b (M1/70), GR-1 (RB6-8C5), TCRβ (H57-597), CD44 (IM7), CD62L (MLE-14), CD45.1 (A20), CD45.2 (104), CD45 (30-F11), B220 (RA3-6B2), CD86/B7-2 (GL-1), and MHCII (I-A^b, AF6-120.1; all from eBioscience or BD); F4/80 (CI:A3-1; AbD Serotec); and anti–mouse neutrophil (7/4; Invitrogen). Biotinylated antibodies were followed by streptavidin-conjugated APC (eBoscience). After the final wash, cells were resuspended in staining/wash buffer containing 1 μg/ml propidium iodide (PI; Sigma-Aldrich) for four-color flow cytometry performed on a FACScan (BD), and data were analyzed with FlowJo software (Tree Star, Inc.). For intracellular analysis of IFN-γ production by T cells by flow cytometry, splenocytes were stimulated for 4 h with 50 ng/ml PMA and 1 μg/ml ionomycin (Sigma-Aldrich) in the presence of 3 μg/ml brefeldin A (eBioscience). Cells were stained extracellularly with PE–conjugated TCRβ, and fixed and permeabilized for intracellular staining with APC-conjugated anti–IFN-γ mAb (XMG1.2; eBioscience). After the final wash, samples were resuspended in staining/washing buffer for flow cytometry analysis performed as described.

Kidney histological analysis and immunofluorescence staining

For each mouse, one kidney was processed for flow cytometric analysis (see the previous section), whereas the other kidney was cut in half laterally. Half of the kidney was fixed in 10% (volume/volume) formalin, embedded in paraffin, and stained with hematoxylin and eosin (H&E) by the UCSF Pathology Core. The other half of the kidney was submerged in optimal cutting temperature embedding media, snap frozen, sectioned (5 μm), and fixed in acetone, and individual sections were stained with FITC-conjugated goat anti–mouse IgG (Fcγ fragment specific) or anti–mouse IgM (μ chain specific; Jackson ImmunoResearch Laboratories, Inc.), or FITC-conjugated anti–mouse C3 (Cappel Laboratories). Images of H&E staining were taken on a microscope (DMLB; Leica) at 400 and 100× magnifications, whereas images of immunofluorescent staining were taken on a microscope (Eclipse TS100; Nikon) at a 200× magnification. The presence and severity of nephritis were determined on H&E-stained sections by an expert pathologist blinded to the mouse genotype. The severity of disease in the glomerular and interstitial compartment was arbitrarily graded as 0 (absent), 1 (mild), 2 (moderate), or 3 (severe). Morphological analysis involved assessment of the following: for glomerulonephritis, glomerular hypercellularity, glomerular size, and presence of glomerual sclerosis; and for interstitial nephritis, infiltration of mononuclear cells and loss of normal architecture. No clear sign of vasculitis was observed in any of the experimental conditions tested. Immunofluorescence intensity of Ig immune complex and C3 deposits were subjectively graded in a blinded analysis as − (absent), + (minimal), ++ (mild), or +++ (severe).

Cytokine assays

BAFF concentrations in sera, cell-free supernatants, and cell-associated pellets were measured by ELISA using cytokine-specific antibodies from R&D (1 μg/ml rat anti–mouse BAFF mAb [clone 121808] and 15 ng/ml biotinylated goat anti–mouse BAFF pAb as coating and detection antibodies, respectively) according to the manufacturer's ELISA protocol. IFN-γ in sera was measured by ELISA using cytokine-specific paired antibodies (BD) according to the manufacturer's protocol.

ANA immunofluorescence

Serum was diluted 1:40 and used for indirect immunofluorescence on fixed Hep-2 ANA slides (Bio-Rad Laboratories), with FITC-conjugated goat anti–mouse IgG (Fcγ fragment specific; Jackson ImmunoResearch Laboratories, Inc.) as the detection reagent. Slides were read on an Eclipse TS100 microscope at a 400× magnification and scored as either a nuclear homogeneous and/or nuclear speckled staining pattern by a reader blinded to the genotype of the mice.

Serum Ig and autoantibody measurement

Levels of serum IgG (total and specific isotypes) and IgM were quantified using ELISA-specific quantification kits (Bethyl Laboratories, Inc.) according to the manufacturer's protocol. For anti-dsDNA Ig ELISA, 96-well flat-bottom plates (Microtest; BD) were coated with 20 ng/well of linearized pUC19 plasmid in 100 mM Tris-HCl. For anti-RNA Ig ELISA, plates (Thermo Fisher Scientific) were coated with 500 U/ml of Smith antigen ribonucleoprotein complex antigen (Sm/RNP Ag; Immunovision) in carbonate buffer, pH 9.5, overnight at 4°C. After overnight incubation, plates were blocked with PBS containing 2% (volume/volume) FBS and 0.05% Tween 20 for 1 h. Serial dilutions of sera were added to the plate and incubated for 2 h at room temperature. The assays were developed with horseradish peroxidase–conjugated goat anti–mouse IgM antibodies (μ chain specific) or anti–mouse IgG (Fc fragment or isotype specific; all from Bethyl Laboratories, Inc.), respectively. After addition of the tetramethylbenzidine substrate (KPL Inc.), the reaction was stopped by adding 1 M phosphoric acid (Sigma-Aldrich), and the absorbance at 450 nm (A_{450}) was measured with a microplate reader (Spectra Max Plus; MDS Analytical Technologies). Results reported are relative to the following serum dilutions: 1:40 for total or isotype-specific IgG and 1:160 for IgM anti-DNA/RNA antibodies; and 1:60,000 for total IgG, 1:25,000 for total IgG1 and Ig2b, 1:12,000 for total IgG3 and IgG2a/c, and 1:20,000 for total IgM antibodies.

Western blotting

Cell lysates prepared as previously described (Mócsai et al., 2006) were run on SDS-PAGE and immunoblotted using antibodies against p-STAT1 (Abcam) and α-actin (Cell Signaling Technology), followed by fluorescence-labeled secondary antibodies detected with the Odyssey Infrared Imaging System (LI-COR Biosciences).

RNA extractions and TaqMan real-time PCR analysis

RNA extractions from purified cells, total spleens, or kidneys were performed using an RNeasy kit (QIAGEN) according to the manufacturer's instructions. Retrotranscription was performed using the iScript cDNA Synthesis Kit (Bio-Rad Laboratories) according to the manufacturer's instructions. Quantitative RT-PCR was performed on a sequence detection instrument (ABI 7700; TaqMan; Applied Biosystems). BAFF and HPRT primer pairs and probes were described previously (Lesley et al., 2004). Other primers pairs and probes used, including their specificity, orientation (F, forward; R, reverse), and sequence were as follows: IFN-γ, (F) 5′-TCAAGTGGCATAGATGTGGAAGAA-3′, (R) 5′-TGGCTCTGCAGGATTTTCATG-3′, and (probe) 5′-TCACCATCCTTTTGCCAGTTCCTCCAG-3′; and CXCL10/IP-10, (F) 5′-ACTGGAGTGAAGCCACGCA-3′, (R) 5′-TGATGGAGAGAGGCTCTCTGC-3′, and (probe) 5′-CCCCGGTGCTGCGATGGATGT-3′. Values of BAFF, IFN-γ, or CXCL10/IP-10 mRNA were normalized to the values of HPRT mRNA in each sample.

B cell survival

Resting mouse splenic B cells were isolated by a B cell isolation kit (Miltenyi Biotec), plated at 4 × 10^5 cells/well, and cultured in RPMI 1640 complete medium (see Cell isolation and culture) containing 2.5 μM β-mercaptoethanol

(Invitrogen) in 96-well tissue culture plates (BD), and incubated at 37°C in 5% CO_2 for 72 h in the presence or absence of the following stimuli: 5 ng/ml recombinant mouse BAFF (Human Genome Sciences), 100 U/ml recombinant mouse IFN-γ, or culture media, conditioned either by WT or $lyn^{-/-}$ BMD DCs stimulated for 48 h with 100 U/ml of recombinant mouse IFN-γ. Each experimental condition was preincubated with 0.5 μg/ml of neutralizing hamster anti-BAFF mAbs (provided by B. Nardelli, Human Genome Sciences, Rockville, MD) or isotype control antibodies (BD) before being added to the B cell culture. Survival of B cells was calculated by flow cytometry analysis on forward/side scatter plots plus the percentage of PI-negative B cells.

ELISPOT

To determine the frequency of antibody-forming cells (AFCs) specific for dsDNA, 96-well filter plates (MultiScreenHTS; Millipore) were coated overnight at 4°C with 10 μg/ml of linearized pUC19 plasmid in 100 mM Tris-HCl. Plates were blocked with PBS containing 1% (weight/volume) BSA (Sigma-Aldrich) for 1 h at 37°C. Freshly isolated splenocytes were resuspended in RPMI 1640 complete medium containing 2% (volume/volume) FBS and 2.5 μM β-mercaptoethanol, plated in duplicate at multiple dilutions (starting with 10^6), and incubated overnight at 37°C in 5% CO_2. 1 μg/ml of biotin-conjugated rat anti–mouse IgM (clone II/41; BD), alkaline phosphatase–conjugated streptavidin (1:500 dilution; KPL Inc.), and BCIP/NBT phosphatase substrate (KPL Inc.) were used for detection. DNA-specific spots were read with an ELISPOT reader (Transtec 1300; AID Diagnostika) and reported as the mean number of AFCs for 10^5 B cells.

Anti–mouse BAFF and recombinant mouse IFN-γ treatment regimens

Anti-BAFF mAb treatment. Long-term anti-BAFF mAb treatment was performed starting from 6–8 wk of age in $lyn^{-/-}$ mice by giving intraperitoneal injections of 2–3 μg/20 g of body weight of neutralizing hamster anti-BAFF mAb (clone 10F4B; provided by Human Genome Sciences; Scholz et al., 2008) or isotype control mAb (BD) every other day for 5 mo. Short-term anti-BAFF mAb treatment was performed under a similar dose/frequency regimen but for 2 mo starting when the mice were 6–7 mo old. To establish the dosing regimen that led to reduced autoreactive B cell clones without inducing a complete depletion of mature B cells, mice were bled every 2–3 wk and serum levels of BAFF, total Ig, and autoantibodies were measured as described in Serum Ig and autoantibody measurement. The percentage of peripheral B cells was analyzed by flow cytometry as described in Flow cytometry (FACS).

rIFN-γ treatment. Starting from 8 wk of age, mice were given intraperitoneal injections of 5×10^4 U rIFN-γ or saline as a control three times weekly for a period of 3 mo. Mice were bled every 2–3 wk and followed up as described for the anti-BAFF mAb treatment.

Adoptive T cell transfers

Resting T cells were isolated from single-cell suspensions of WT (CD45.1/2 het) or *BAFF-R*$^{-/-}$ (CD45.2) mouse spleens and lymph nodes using a T cell isolation kit (Miltenyi Biotec) according to manufacturer's instructions. Purified WT or *BAFF-R*$^{-/-}$ T cells were mixed in a 1:1 ratio, and a total of 1.2×10^7 cells in 200 μl of saline solution were injected i.v. into 6–7-mo-old WT or $lyn^{-/-}$ mice (CD45.1). 15 d after transfer, the spleens of host mice were harvested and the levels of T cell activation and IFN-γ production in host and donor T cells were analyzed by taking advantage of the differential expression of the CD45.1/2 markers by flow cytometry, as described in Flow cytometry (FACS).

Statistical analysis

Significance was determined with the unpaired two-tailed Student's *t* test.

Online supplemental material

Fig. S1 depicts excessive proliferation, enhanced IFN-γ responses, and increased BAFF release by Lyn-deficient myeloid cells. Fig. S2 shows that BAFF produced by $lyn^{-/-}$ myeloid cells is biologically active. Fig. S3 shows that the genetic deletion of Hck/Fgr reduces myeloproliferation in $lyn^{-/-}$ mice, whereas production of autoreactive autoantibodies and B cell hyperactivation are not affected. Fig. S4 shows that $lyn^{-/-}rag^{-/-}$-WT chimeras develop myeloproliferation and increased amounts of autoreactive IgM in the sera. Fig. S5 shows that genetic deletion of IFN-γ reduces myeloproliferation as well as IgG immune complex and C3 deposits in the kidneys in $lyn^{-/-}$ mice. Fig. S6 shows that IFN-γ deficiency in the lymphoid compartment reduces BAFF serum levels, blocks splenomegaly, and improves autoimmunity in $lyn^{-/-}rag^{-/-}$ -WT chimeras. Fig. S7 depicts the effect of long-term anti-BAFF mAb treatment on $lyn^{-/-}$ B cell subtypes and hyperactivation, IFN-γ serum levels, and Ig immune complex and C3 deposits in the kidneys. Fig. S8 depicts the effect of short-term anti-BAFF mAb treatment on $lyn^{-/-}$ B cell subtypes and hyperactivation. Online supplemental material is available at http://www.jem.org/cgi/content/full/jem.20100086/DC1.

We thank C. Abram, A. Gross, M. Hermsiton, M.J. Bluestone, M. Anderson, and M. Klinger for suggestions and comments, and F. Chanut for manuscript criticism. B. Nardelli (formerly of Human Genome Sciences) provided initial lots of anti-BAFF mAb.

This work was supported by the National Institutes of Health (grants AI65495 and AI68150 to C.A. Lowell, and grant AI078869 to A.L. DeFranco) and the Fondazione Cariverona (P. Scapini).

The authors have no conflicting financial interests.

Submitted: 12 January 2010
Accepted: 10 June 2010

REFERENCES

Bagavant, H., and S.M. Fu. 2005. New insights from murine lupus: disassociation of autoimmunity and end organ damage and the role of T cells. *Curr. Opin. Rheumatol.* 17:523–528. doi:10.1097/01.bor.0000169361.23325.1e

Balomenos, D., R. Rumold, and A.N. Theofilopoulos. 1998. Interferon-gamma is required for lupus-like disease and lymphoaccumulation in MRL-lpr mice. *J. Clin. Invest.* 101:364–371. doi:10.1172/JCI750

Berton, G., A. Mócsai, and C.A. Lowell. 2005. Src and Syk kinases: key regulators of phagocytic cell activation. *Trends Immunol.* 26:208–214. doi:10.1016/j.it.2005.02.002

Cash, H., M. Relle, J. Menke, C. Brochhausen, S.A. Jones, N. Topley, P.R. Galle, and A. Schwarting. 2010. Interleukin 6 (IL-6) deficiency delays lupus nephritis in MRL-Faslpr mice: the IL-6 pathway as a new therapeutic target in treatment of autoimmune kidney disease in systemic lupus erythematosus. *J. Rheumatol.* 37:60–70. doi:10.3899/jrheum.090194

Chan, V.W., F. Meng, P. Soriano, A.L. DeFranco, and C.A. Lowell. 1997. Characterization of the B lymphocyte populations in Lyn-deficient mice and the role of Lyn in signal initiation and down-regulation. *Immunity.* 7:69–81. doi:10.1016/S1074-7613(00)80511-7

Chan, V.W., C.A. Lowell, and A.L. DeFranco. 1998. Defective negative regulation of antigen receptor signaling in Lyn-deficient B lymphocytes. *Curr. Biol.* 8:545–553. doi:10.1016/S0960-9822(98)70223-4

Chan, O.T., L.G. Hannum, A.M. Haberman, M.P. Madaio, and M.J. Shlomchik. 1999. A novel mouse with B cells but lacking serum antibody reveals an antibody-independent role for B cells in murine lupus. *J. Exp. Med.* 189:1639–1648. doi:10.1084/jem.189.10.1639

Chu, C.L., and C.A. Lowell. 2005. The Lyn tyrosine kinase differentially regulates dendritic cell generation and maturation. *J. Immunol.* 175:2880–2889.

Cohen, P.L., R. Caricchio, V. Abraham, T.D. Camenisch, J.C. Jennette, R.A. Roubey, H.S. Earp, G. Matsushima, and E.A. Reap. 2002. Delayed apoptotic cell clearance and lupus-like autoimmunity in mice lacking the c-mer membrane tyrosine kinase. *J. Exp. Med.* 196:135–140. doi:10.1084/jem.20012094

Ding, C. 2008. Belimumab, an anti-BLyS human monoclonal antibody for potential treatment of inflammatory autoimmune diseases. *Expert Opin. Biol. Ther.* 8:1805–1814. doi:10.1517/14712598.8.11.1805

Dörner, T., A. Radbruch, and G.R. Burmester. 2009. B-cell-directed therapies for autoimmune disease. *Nat. Rev. Rheumatol.* 5:433–441. doi:10.1038/nrrheum.2009.141

Ettinger, R., G.P. Sims, R. Robbins, D. Withers, R.T. Fischer, A.C. Grammer, S. Kuchen, and P.E. Lipsky. 2007. IL-21 and BAFF/BLyS

synergize in stimulating plasma cell differentiation from a unique population of human splenic memory B cells. *J. Immunol.* 178:2872–2882.

Gross, A.J., J.R. Lyandres, A.K. Panigrahi, E.T. Prak, and A.L. DeFranco. 2009. Developmental acquisition of the Lyn-CD22-SHP-1 inhibitory pathway promotes B cell tolerance. *J. Immunol.* 182:5382–5392. doi:10.4049/jimmunol.0803941

Hamilton, J.A. 2008. Colony-stimulating factors in inflammation and autoimmunity. *Nat. Rev. Immunol.* 8:533–544. doi:10.1038/nri2356

Hanada, T., H. Yoshida, S. Kato, K. Tanaka, K. Masutani, J. Tsukada, Y. Nomura, H. Mimata, M. Kubo, and A. Yoshimura. 2003. Suppressor of cytokine signaling-1 is essential for suppressing dendritic cell activation and systemic autoimmunity. *Immunity*. 19:437–450. doi:10.1016/S1074-7613(03)00240-1

Harder, K.W., L.M. Parsons, J. Armes, N. Evans, N. Kountouri, R. Clark, C. Quilici, D. Grail, G.S. Hodgson, A.R. Dunn, and M.L. Hibbs. 2001. Gain- and loss-of-function Lyn mutant mice define a critical inhibitory role for Lyn in the myeloid lineage. *Immunity*. 15:603–615. doi:10.1016/S1074-7613(01)00208-4

Harder, K.W., C. Quilici, E. Naik, M. Inglese, N. Kountouri, A. Turner, K. Zlatic, D.M. Tarlinton, and M.L. Hibbs. 2004. Perturbed myelo/erythropoiesis in Lyn-deficient mice is similar to that in mice lacking the inhibitory phosphatases SHP-1 and SHIP-1. *Blood*. 104:3901–3910. doi:10.1182/blood-2003-12-4396

Harigai, M., M. Kawamoto, M. Hara, T. Kubota, N. Kamatani, and N. Miyasaka. 2008. Excessive production of IFN-gamma in patients with systemic lupus erythematosus and its contribution to induction of B lymphocyte stimulator/B cell-activating factor/TNF ligand superfamily-13B. *J. Immunol.* 181:2211–2219.

Hibbs, M.L., D.M. Tarlinton, J. Armes, D. Grail, G. Hodgson, R. Maglitto, S.A. Stacker, and A.R. Dunn. 1995. Multiple defects in the immune system of Lyn-deficient mice, culminating in autoimmune disease. *Cell*. 83:301–311. doi:10.1016/0092-8674(95)90171-X

Huard, B., P. Schneider, D. Mauri, J. Tschopp, and L.E. French. 2001. T cell costimulation by the TNF ligand BAFF. *J. Immunol.* 167:6225–6231.

Kalled, S.L. 2005. The role of BAFF in immune function and implications for autoimmunity. *Immunol. Rev.* 204:43–54. doi:10.1111/j.0105-2896.2005.00219.x

Kaneko, Y., F. Nimmerjahn, M.P. Madaio, and J.V. Ravetch. 2006. Pathology and protection in nephrotoxic nephritis is determined by selective engagement of specific Fc receptors. *J. Exp. Med.* 203:789–797. doi:10.1084/jem.20051900

Lai Kwan Lam, Q., O. King Hung Ko, B.J. Zheng, and L. Lu. 2008. Local BAFF gene silencing suppresses Th17-cell generation and ameliorates autoimmune arthritis. *Proc. Natl. Acad. Sci. USA*. 105:14993–14998. doi:10.1073/pnas.0806044105

Lesley, R., Y. Xu, S.L. Kalled, D.M. Hess, S.R. Schwab, H.B. Shu, and J.G. Cyster. 2004. Reduced competitiveness of autoantigen-engaged B cells due to increased dependence on BAFF. *Immunity*. 20:441–453. doi:10.1016/S1074-7613(04)00079-2

Liang, B., D.B. Gardner, D.E. Griswold, P.J. Bugelski, and X.Y. Song. 2006. Anti-interleukin-6 monoclonal antibody inhibits autoimmune responses in a murine model of systemic lupus erythematosus. *Immunology*. 119:296–305. doi:10.1111/j.1365-2567.2006.02433.x

Lowell, C.A. 2004. Src-family kinases: rheostats of immune cell signaling. *Mol. Immunol.* 41:631–643. doi:10.1016/j.molimm.2004.04.010

Mackay, F., and H. Leung. 2006. The role of the BAFF/APRIL system on T cell function. *Semin. Immunol.* 18:284–289. doi:10.1016/j.smim.2006.04.005

Mackay, F., and P. Schneider. 2009. Cracking the BAFF code. *Nat. Rev. Immunol.* 9:491–502. doi:10.1038/nri2572

Mackay, F., P.A. Silveira, and R. Brink. 2007. B cells and the BAFF/APRIL axis: fast-forward on autoimmunity and signaling. *Curr. Opin. Immunol.* 19:327–336. doi:10.1016/j.coi.2007.04.008

Maeda, K., A. Malykhin, B.N. Teague-Weber, X.H. Sun, A.D. Farris, and K.M. Coggeshall. 2009. Interleukin-6 aborts lymphopoiesis and elevates production of myeloid cells in systemic lupus erythematosus-prone B6.Sle1.Yaa animals. *Blood*. 113:4534–4540. doi:10.1182/blood-2008-12-192559

Meng, F., and C.A. Lowell. 1997. Lipopolysaccharide (LPS)-induced macrophage activation and signal transduction in the absence of Src-family kinases Hck, Fgr, and Lyn. *J. Exp. Med.* 185:1661–1670. doi:10.1084/jem.185.9.1661

Mócsai, A., C.L. Abram, Z. Jakus, Y. Hu, L.L. Lanier, and C.A. Lowell. 2006. Integrin signaling in neutrophils and macrophages uses adaptors containing immunoreceptor tyrosine-based activation motifs. *Nat. Immunol.* 7:1326–1333. doi:10.1038/ni1407

Moisini, I., and A. Davidson. 2009. BAFF: a local and systemic target in autoimmune diseases. *Clin. Exp. Immunol.* 158:155–163. doi:10.1111/j.1365-2249.2009.04007.x

Ng, L.G., A.P. Sutherland, R. Newton, F. Qian, T.G. Cachero, M.L. Scott, J.S. Thompson, J. Wheway, T. Chtanova, J. Groom, et al. 2004. B cell-activating factor belonging to the TNF family (BAFF)-R is the principal BAFF receptor facilitating BAFF costimulation of circulating T and B cells. *J. Immunol.* 173:807–817.

Ng, L.G., C.R. Mackay, and F. Mackay. 2005. The BAFF/APRIL system: life beyond B lymphocytes. *Mol. Immunol.* 42:763–772. doi:10.1016/j.molimm.2004.06.041

Nishizumi, H., I. Taniuchi, Y. Yamanashi, D. Kitamura, D. Ilic, S. Mori, T. Watanabe, and T. Yamamoto. 1995. Impaired proliferation of peripheral B cells and indication of autoimmune disease in lyn-deficient mice. *Immunity*. 3:549–560. doi:10.1016/1074-7613(95)90126-4

Pereira, S., and C. Lowell. 2003. The Lyn tyrosine kinase negatively regulates neutrophil integrin signaling. *J. Immunol.* 171:1319–1327.

Rahman, A., and D.A. Isenberg. 2008. Systemic lupus erythematosus. *N. Engl. J. Med.* 358:929–939. doi:10.1056/NEJMra071297

Ramanujam, M., and A. Davidson. 2008. BAFF blockade for systemic lupus erythematosus: will the promise be fulfilled? *Immunol. Rev.* 223:156–174. doi:10.1111/j.1600-065X.2008.00625.x

Ramanujam, M., X. Wang, W. Huang, Z. Liu, L. Schiffer, H. Tao, D. Frank, J. Rice, B. Diamond, K.O. Yu, et al. 2006. Similarities and differences between selective and nonselective BAFF blockade in murine SLE. *J. Clin. Invest.* 116:724–734. doi:10.1172/JCI26385

Rane, S.G., and E.P. Reddy. 2002. JAKs, STATs and Src kinases in hematopoiesis. *Oncogene*. 21:3334–3358. doi:10.1038/sj.onc.1205398

Sarantopoulos, S., K.E. Stevenson, H.T. Kim, N.S. Bhuiya, C.S. Cutler, R.J. Soiffer, J.H. Antin, and J. Ritz. 2007. High levels of B-cell activating factor in patients with active chronic graft-versus-host disease. *Clin. Cancer Res.* 13:6107–6114. doi:10.1158/1078-0432.CCR-07-1290

Scapini, P., F. Bazzoni, and M.A. Cassatella. 2008. Regulation of B-cell-activating factor (BAFF)/B lymphocyte stimulator (BLyS) expression in human neutrophils. *Immunol. Lett.* 116:1–6.

Scapini, P., S. Pereira, H. Zhang, and C.A. Lowell. 2009. Multiple roles of Lyn kinase in myeloid cell signaling and function. *Immunol. Rev.* 228:23–40. doi:10.1111/j.1600-065X.2008.00758.x

Schneider, P. 2005. The role of APRIL and BAFF in lymphocyte activation. *Curr. Opin. Immunol.* 17:282–289. doi:10.1016/j.coi.2005.04.005

Scholz, J.L., J.E. Crowley, M.M. Tomayko, N. Steinel, P.J. O'Neill, W.J. Quinn III, R. Goenka, J.P. Miller, Y.H. Cho, V. Long, et al. 2008. BLyS inhibition eliminates primary B cells but leaves natural and acquired humoral immunity intact. *Proc. Natl. Acad. Sci. USA*. 105:15517–15522. doi:10.1073/pnas.0807841105

Shlomchik, M.J., J.E. Craft, and M.J. Mamula. 2001. From T to B and back again: positive feedback in systemic autoimmune disease. *Nat. Rev. Immunol.* 1:147–153. doi:10.1038/35100573

Silver, K.L., T.L. Crockford, T. Bouriez-Jones, S. Milling, T. Lambe, and R.J. Cornall. 2007. MyD88-dependent autoimmune disease in Lyn-deficient mice. *Eur. J. Immunol.* 37:2734–2743. doi:10.1002/eji.200737293

Stadanlick, J.E., and M.P. Cancro. 2008. BAFF and the plasticity of peripheral B cell tolerance. *Curr. Opin. Immunol.* 20:158–161. doi:10.1016/j.coi.2008.03.015

Stohl, W., D. Xu, K.S. Kim, M.N. Koss, T.N. Jorgensen, B. Deocharan, T.E. Metzger, S.A. Bixler, Y.S. Hong, C.M. Ambrose, et al. 2005. BAFF overexpression and accelerated glomerular disease in mice with an incomplete genetic predisposition to systemic lupus erythematosus. *Arthritis Rheum.* 52:2080–2091. doi:10.1002/art.21138

Stranges, P.B., J. Watson, C.J. Cooper, C.M. Choisy-Rossi, A.C. Stonebraker, R.A. Beighton, H. Hartig, J.P. Sundberg, S. Servick, G. Kaufmann, et al. 2007. Elimination of antigen-presenting cells and

autoreactive T cells by Fas contributes to prevention of autoimmunity. *Immunity*. 26:629–641. doi:10.1016/j.immuni.2007.03.016

Sutherland, A.P., L.G. Ng, C.A. Fletcher, B. Shum, R.A. Newton, S.T. Grey, M.S. Rolph, F. Mackay, and C.R. Mackay. 2005. BAFF augments certain Th1-associated inflammatory responses. *J. Immunol.* 174:5537–5544.

Theofilopoulos, A.N., S. Koundouris, D.H. Kono, and B.R. Lawson. 2001. The role of IFN-gamma in systemic lupus erythematosus: a challenge to the Th1/Th2 paradigm in autoimmunity. *Arthritis Res.* 3:136–141. doi:10.1186/ar290

Tsantikos, E., S.A. Oracki, C. Quilici, G.P. Anderson, D.M. Tarlinton, and M.L. Hibbs. 2009. Autoimmune disease in Lyn-deficient mice is dependent on an inflammatory environment established by IL-6. *J. Immunol.* 184:1348–1360.

Xu, Y., K.W. Harder, N.D. Huntington, M.L. Hibbs, and D.M. Tarlinton. 2005. Lyn tyrosine kinase: accentuating the positive and the negative. *Immunity*. 22:9–18.

Yanaba, K., J.D. Bouaziz, T. Matsushita, C.M. Magro, E.W. St.Clair, and T.F. Tedder. 2008. B-lymphocyte contributions to human autoimmune disease. *Immunol. Rev.* 223:284–299. doi:10.1111/j.1600-065X.2008.00646.x

Ye, Q., L. Wang, A.D. Wells, R. Tao, R. Han, A. Davidson, M.L. Scott, and W.W. Hancock. 2004. BAFF binding to T cell-expressed BAFF-R costimulates T cell proliferation and alloresponses. *Eur. J. Immunol.* 34:2750–2759. doi:10.1002/eji.200425198

Yu, C.C., T.S. Yen, C.A. Lowell, and A.L. DeFranco. 2001. Lupus-like kidney disease in mice deficient in the Src family tyrosine kinases Lyn and Fyn. *Curr. Biol.* 11:34–38. doi:10.1016/S0960-9822(00)00024-5

Zhu, J., X. Liu, C. Xie, M. Yan, Y. Yu, E.S. Sobel, E.K. Wakeland, and C. Mohan. 2005. T cell hyperactivity in lupus as a consequence of hyperstimulatory antigen-presenting cells. *J. Clin. Invest.* 115:1869–1878. doi:10.1172/JCI23049